IN THE UNITED STATES PATENT AND TRADEMARK OFFICE
BEFORE THE BOARD OF PATENT APPEALS AND INTERFERENCES

In re Application of	
SPAMPINATO, et al.	Art Unit: 2855
Serial Number 10/797,600	Examiner: Bonanto, G.
Filed: March 11, 2004	Attorney Reference: 005127.00270
For: TESTING APPARATUS	

APPEAL BRIEF

Commissioner for Patents
U.S. Patent and Trademark Office
Alexandria, VA 22313

Sir:

Appellants hereby appeal to the Board of Patent Appeals and Interferences from the decision of the Primary Examiner finally rejecting claims 10-12, 14-17, and 34-38 in the above-captioned patent application.

I. Real Party In Interest

The real party in interest is Nike, Inc., a corporation organized and existing under the laws of the State of Oregon in the United States of America, and having its principal place of business at One Bowerman Drive, Beaverton, Oregon 97005.

II. Related Appeals and Interferences

Appellants and the legal representative of the Appellants are unaware of any appeals or interferences related to the subject appeal.

III. Status of Claims

Claims 10-12, 14-17, and 34-38 (reproduced for reference in a Claims Appendix attached hereto) are pending in the application. Each of claims 10-12, 14-17, and 34-38 stand rejected, as outlined in a final Office Action mailed December 28, 2005 and an Advisory Action mailed March 29, 2006. Appellants hereby appeal the final rejection of claims 10-12, 14-17, and 34-38.

IV. Status of Amendments

In an Amendment filed March 12, 2006 in response to the final Office Action, claim 10 was amended to recite a rounded leading edge and a tapered trailing edge. According to the Advisory Action, the amendment will be entered for purposes of appeal.

V. Summary of Claimed Subject Matter

Aspects of the invention include a testing apparatus for a game ball. With reference to Figures 1 and 2 of the application, the testing apparatus is depicted as having a housing 20, a shaft 30, a mount 40, a motor 50, and a sensor 60. In general, housing 20 extends into a wind tunnel during the testing of a game ball 100. Shaft 30 extends through housing 20 and is rotatable. A first end portion of shaft 30 is secured to mount 40 such that mount 40 rotates with shaft 30. An opposite second end portion of shaft 30 is operatively connected to motor 50, which induces rotation in shaft 30 and mount 40. Mount 40, which also extends into the wind tunnel, is configured to support game ball 100 and secure game ball 100 to the testing apparatus. Motor 50 may be any device suitable for rotating shaft 30 and mount 40, and motor 50 may include a gear reducer for increasing the angular velocity of shaft 30 and mount 40. Sensor 60 detects various forces upon shaft 30, which translate into the fluid forces upon game ball 100. Accordingly, testing apparatus 10 rotates game ball 100 within a wind tunnel and detects various fluid forces upon game ball 100 due to movement of a fluid (i.e., air) within the wind tunnel. (Application, page 7, line 28 through page 8, line 14).

The overall shape of housing 20 may vary significantly to include any suitable airfoil configuration, including the configuration of a National Advisory Committee on Aeronautics (NACA) 4-digit series airfoil. Referring to the cross-sections of Figures 8A-8C, the airfoil configuration of housing 20 generally forms the shape of a tear drop that is consistent with an air

foil shape. That is, leading edge 25 exhibits a generally rounded shape that tapers to a pointed shape at trailing edge 26. (Application, page 8, line 26 through page 9, line 9).

VI. Grounds of Rejection to be Reviewed on Appeal

The following rejections of claims 10-12, 14-17, and 34-38 were submitted by the Examiner in the final Office Action:

- Claims 10-12, 14, 16, and 17 are rejected under 35 U.S.C. §103(a) as being unpatentable over a combination of U.S. Patent Number 6,571,618 to Demay, et al., U.S. Patent Number 3,306,101 to Holderer, and a publication entitled *The Aerodynamics of a Tennis Ball* by Mehta, et al.;
- Claim 15 is rejected under 35 U.S.C. §103(a) as being unpatentable over a combination of Demay, Holderer, and a publication entitled *Golf Ball Aerodynamics* by Bearman, et al.;
- Claims 34 and 35 are rejected under 35 U.S.C. §103(a) as being unpatentable over a combination of Demay, Holderer, and U.S. Patent Number 4,501,214 to Meyer;
- Claim 36 is rejected under 35 U.S.C. §103(a) as being unpatentable over a combination of Demay, Holderer, Meyer, and Bearman; and
- Claims 37 and 38 are rejected under 35 U.S.C. §103(a) as being unpatentable over a combination of Demay, Holderer, Meyer, and Mehta.

The Demay, Holderer, Mehta, Bearman, and Meyer references are respectively reproduced for reference in Evidence Appendices A, B, C, D, and E attached hereto.

VII. Argument

Discussion of Claims 10-12 and 14-17

Independent claim 10 recites a testing apparatus for a game ball. The testing apparatus includes a rotating element, a mount, an airfoil, and a sensor. The rotating element has a first end, a second end, and a longitudinal axis that extends through the first end and the second end. In addition, the rotating element is rotatable about the longitudinal axis. The mount is located proximal the first end of the rotating element and configured to secure to the game ball. The mount is rotatable with the rotating element about the longitudinal axis. The airfoil extends around the rotating element, and the airfoil has a rounded leading edge and a tapered trailing

edge. The sensor detects forces upon the game ball in a first direction and a second direction. The first direction corresponds with a direction between the leading edge and the trailing edge, and the second direction is orthogonal to both the first direction and the longitudinal axis.

The Office Action rejects independent claim 10 as being unpatentable over Demay, Holderer, and Mehta. To establish obviousness, the burden is upon the Examiner to demonstrate that the prior art references teach or suggest all claim limitations. That is, all of the claim limitations must be taught or suggested by the prior art. *In re Royka*, 490 F.2d 981 (C.C.P.A. 1974). None of the prior art references cited by the Examiner against independent claim 10, however, disclose (a) an airfoil or (b) a rounded leading edge and a tapered trailing edge.

According to the rejection, Demay discloses an airfoil extending around the rotating element, and the airfoil has a leading edge and a trailing edge (i.e., the casing 44 in Figure 3). The mere fact that the casing is streamlined, according to the Examiner, does not indicate that the casing is an airfoil. Every round object does not qualify as a sphere. Similarly, every streamlined object does not qualify as an airfoil. An airfoil is a term of art that denotes a particular shape with the ability to control stability, direction, lift, thrust, or propulsion, for example. Whereas independent claim 10 recites the presence of an airfoil, Demay merely discloses a streamlined casing without the qualities of an airfoil. Furthermore, the casing does not have a rounded leading edge and a tapered trailing edge.

Based upon the above discussion, the Applicants respectfully submit that independent claim 10 is allowable over Demay, Holderer, and Mehta. In addition, claims 11, 12, 14, 16, and 17 should be allowable for at least the same reasons. Claim 15 should also be allowable as Bearman does not remedy the deficiencies discussed above.

Discussion of Claims 34-36

Independent claim 34 recites a testing apparatus for a game ball. The testing apparatus includes a rotating element, a mount, a support, and a sensor. The rotating element has a first end, a second end, and a longitudinal axis that extends through the first end and the second end. In addition, the rotating element is rotatable about the longitudinal axis. The mount is located proximal the first end of the rotating element and configured to secure to the game ball. The mount is rotatable with the rotating element about the longitudinal axis. The support extends around the rotating element, and the support has a rounded leading edge and a tapered trailing

edge that define a teardrop shape in the support. The sensor detects forces upon the game ball in a first direction and a second direction. The first direction corresponds with a direction between the leading edge and the trailing edge, and the second direction is orthogonal to both the first direction and the longitudinal axis.

The Office Action rejects independent claim 10 as being unpatentable over Demay, Holderer, and Meyer.

i. No Prima Facie Case

To establish a *prima facie* case of obviousness, the burden is upon the Examiner to demonstrate reasons why a skilled artisan, confronted with the same problem as the inventor and with no knowledge of the claimed invention, would select the elements from the cited prior art references for combination in the manner claimed. *In re Rouffet*, 149 F.3d 1350, 1357, 47 U.S.P.Q.2d 1453, 1458 (Fed. Cir. 1998). Accordingly, obviousness cannot be established by combining the teachings of the prior art to produce the claimed invention, absent some teaching, suggestion, or incentive supporting the combination. *In re Geiger*, 815 F.2d 686, 688, 2 U.S.P.Q.2d 1276, 1278 (Fed. Cir. 1987). With regard to the present issue, the rejection does not establish a *prima facie* case of obviousness because no proper motivation exists to combine Demay, Holderer, and Meyer.

As a motivation for making the combination of Demay, Holderer, and Meyer, the rejection states that it would have been obvious to "modify the streamlined casing of Demay et al. by making it tear-drop shape as taught by Meyer in order to make the support strong and light" (Office Action, page 9, final 3 lines). As a first matter, there is no showing or even an attempt to demonstrate that a combination of Demay, Holderer, and Meyer would actually provide a stronger or lighter support. That is, the rejection merely asserts that the combination would increase strength and decrease weight without any attempt to actually demonstrate that strength would be increased or weight would be decreased. Furthermore, the rejection fails to demonstrate that a teaching, suggestion, or incentive supporting the combination exists. Neither Demay, Holderer, nor Meyer discuss a need for increasing strength and decreasing weight of a support, and the Appellant is aware of no recognized understanding in the art that the devices of Demay and Holderer are in need of changes in strength and weight. Accordingly, the rejection of independent claim 34 is improper for failing to establish a *prima facie* case of obviousness.

ii. Unsatisfactory For Intended Purpose

If a proposed modification would render the prior art invention being modified unsatisfactory for its intended purpose, then there is no suggestion or motivation to make the proposed modification. *In re Gordon* 733 F.2d 900, 902, 221 U.S.P.Q. 1125, 1127 (Fed. Cir. 1984). As noted above, the rejection states that it would have been obvious to "modify the streamlined casing of Demay et al. by making it tear-drop shape as taught by Meyer in order to make the support strong and light" (Office Action, page 9, final 3 lines). Decreasing the weight of a support for a testing apparatus may actually be detrimental to the performance of the testing apparatus. As air flows around the testing apparatus, the air may tend to move, vibrate, or otherwise affect the testing apparatus, particularly if the testing apparatus is light. Accordingly, decreasing the weight may make the testing apparatuses in Demay and Holderer unsatisfactory for its intended purpose.

iii. Hindsight: Picking and Choosing

Obviousness cannot be established by combining the teachings of the prior art to produce the claimed invention, absent some teaching, suggestion, or incentive supporting the combination. *In re Geiger*, 815 F.2d 686, 688, 2 U.S.P.Q.2d 1276, 1278 (Fed. Cir. 1987). Furthermore, selective hindsight is no more applicable to the design of experiments than it is to the combination of prior art teachings. There must be a reason or suggestion in the art for selecting the procedure used, other than the knowledge learned from the Applicants' disclosure. *In re Dow Chemical Co.*, 837 F.2d 469, 5 U.S.P.Q.2d 1529 (Fed. Cir. 1988). Moreover, hindsight analysis is clearly improper since the statutory test is whether the subject matter as a whole would have been obvious at the time the invention was made. *In Re Deminski*, 796 F.2d 436, 230 U.S.P.Q. 313 (Fed. Cir. 1986).

Demay and Holderer disclose wind tunnel testing apparatuses, and Meyer discloses a mast for a sail. In rejecting independent claim 34, the Office Action merely presents elements from each reference and combines the elements to purportedly arrive at the claimed invention.

The rejection of independent claim 34 does not present a line of reasoning as to why an artisan reviewing only the collective teachings of the references would have found it obvious to selectively pick and choose concepts from Meyer to incorporate into Demay and Holderer. As discussed above, the rationale presented in the Office Action could actually have a detrimental

effect upon the performance of the testing apparatuses in Demay and Holderer. In this circumstance, the rejection does little more than cite references to show that various concepts, when each is viewed in a vacuum, are known. The claimed invention, however, is clearly directed to a combination of concepts (e.g., testing apparatus having rotating element, a mount, a support with a teardrop shape, and a sensor). That is to say, the Applicant does not claim the invention of a teardrop-shaped element, for example, but has presented claims to an invention that is a new combination of concepts. To support the conclusion that the claimed combination is directed to obvious subject matter, the references must expressly or impliedly suggest the claimed combination, or the rejection must present a convincing line of reasoning as to why the artisan would have found the claimed invention to have been obvious in light of the teachings of the references. A review of Demay, Holderer, Meyer, and the Office Action does not provide a sufficient basis that would expressly or impliedly teach or suggest the combinations suggested by the Examiner. More particularly, the rejection of independent claim 34 does not set forth a reasonable motivation for combining Demay, Holderer, and Meyer in a manner that forms a testing apparatus having the features of independent claim 34.

Based upon the above discussion, the Applicants respectfully submit that independent claim 34 is allowable over Demay, Holderer, and Meyer. In addition, claims 35-38 should be allowable for at least the same reasons and because Bearman and Mehta do not remedy the deficiencies discussed above.

Conclusion

The Applicants respectfully submit that rejections submitted in the final Office Action mailed December 28, 2005 and the subsequent Advisory Action mailed March 29, 2006 should be reversed for at least the reasons recited above. Allowance of claims 10-12, 14-17, and 34-38 is, therefore, respectfully requested.

In accordance with 37 C.F.R. §41.31 Appellants submit this Appeal Brief to the Board of Patent Appeals and Interferences. Filed concurrently herewith is a Notice of Appeal and a one month Petition For Extension of Time. Accordingly, the Commissioner is authorized to charge the following fees:

(a) $500 for filing this Appeal Brief;

(b) $500 for the Notice of Appeal; and

(c) $120 for the Petition For Extension of Time.

It is believed that no additional fees are due in connection with this Appeal Brief. Should additional fees be deemed necessary, however, such fees are hereby requested and the Commissioner is authorized to charge deposit account number 19-0733 for the payment of the requisite fee.

Respectfully submitted,

By: Byron S. Kuzara
Registration No. 51,255

Banner & Witcoff, Ltd.
1001 G Street, N.W.
Washington, D.C. 20001-4597
Telephone: (503) 425-6800

Dated: April 28, 2006

Claims Appendix
Claims Involved in the Appeal

1-9. (Cancelled)

10. A testing apparatus for a game ball, the testing apparatus comprising:

a rotating element with a first end, a second end, and a longitudinal axis that extends through the first end and the second end, the rotating element being rotatable about the longitudinal axis;

a mount located proximal the first end of the rotating element and configured to secure to the game ball, the mount being rotatable with the rotating element about the longitudinal axis;

an airfoil extending around the rotating element, the airfoil having a rounded leading edge and a tapered trailing edge; and

a sensor that detects forces upon the game ball in a first direction and a second direction, the first direction corresponding with a direction between the leading edge and the trailing edge, and the second direction being orthogonal to both the first direction and the longitudinal axis.

11. The testing apparatus recited in claim 10, wherein the airfoil has a leading edge and the trailing edge, the airfoil being tapered between the leading edge and the trailing edge.

12. The testing apparatus recited in claim 11, wherein the airfoil is tapered in an area that is between the first end and the second end of the rotating element.

13. (Cancelled)

14. The testing apparatus recited in claim 10, wherein the mount is secured to the first end of the rotating element.

15. The testing apparatus recited in claim 10, wherein a tachometer is operatively connected to the rotating element and detects an angular velocity of the rotating element.

16. The testing apparatus recited in claim 10, wherein the testing apparatus further includes a motor that is operatively connected to the rotating element through a gear reducer.

17. The testing apparatus recited in claim 10, wherein the mount has a concave surface with a curvature that is substantially similar to a curvature of the game ball.

18-33. (Cancelled)

34. A testing apparatus for a game ball, the testing apparatus comprising:

a rotating element with a first end, a second end, and a longitudinal axis that extends through the first end and the second end, the rotating element being rotatable about the longitudinal axis;

a mount located proximal the first end of the rotating element and configured to secure to the game ball, the mount being rotatable with the rotating element about the longitudinal axis;

a support extending around the rotating element, the support having a rounded leading edge and a tapered trailing edge that define a teardrop shape in the support; and

a sensor that detects forces upon the game ball in a first direction and a second direction, the first direction corresponding with a direction between the leading edge and the trailing edge, and the second direction being orthogonal to both the first direction and the longitudinal axis.

35. The testing apparatus recited in claim 34, wherein the mount is secured to the first end of the rotating element.

36. The testing apparatus recited in claim 34, wherein a tachometer is operatively connected to the rotating element and detects an angular velocity of the rotating element.

37. The testing apparatus recited in claim 34, wherein the testing apparatus further includes a motor that is operatively connected to the rotating element.

38. The testing apparatus recited in claim 34, wherein the mount has a concave surface with a curvature that is substantially similar to a curvature of the game ball.

Evidence Appendix A
U.S. Patent Number 6,571,618 to Demay, et al.

This reference was originally entered in the record by the Primary Examiner in an Office Action mailed July 28, 2005.

The aerodynamics of a tennis ball

R. D. Mehta[1] and J. M. Pallis[2]

[1]NASA Ames Research Center, Moffett Field, California, USA
[2]Cislunar Aerospace, Inc., San Francisco, California, USA

Abstract

The aerodynamics of a tennis ball are presented and discussed here with the aid of recent wind tunnel measurements. A flow visualization study was conducted on a 28-cm diameter tennis ball model to establish the boundary layer separation locations and Reynolds number effects for both nonspinning and spinning cases. The flow visualization results showed that the separation location on a nonspinning tennis ball occurred relatively early, near the apex, and appeared very similar to a laminar separation in the subcritical Reynolds number regime. Qualitatively, the flow regime (boundary layer separation location) appeared to be independent of Reynolds number in the range, $167\,000 < Re < 284\,000$. Asymmetric boundary layer separation and a deflected wake flow, depicting the Magnus effect, were observed for the spinning ball. In the second phase of the experiments, the drag coefficient of a variety of new and used tennis balls, including prototypes of the recently approved oversized ball, was measured for the case simulating a perfectly flat serve (a serve with zero spin). The measurements were conducted in a Reynolds number range of about $80\,000 < Re < 300\,000$, which corresponds to a velocity range of $19 < U < 70$ m s^{-1} ($43 < U < 157$ mph). The present data, which indicate relatively high drag coefficients for new tennis balls ($C_D \cong 0.6$–0.7), are compared to existing data for spherical models with varying degrees of surface roughness. The observed (unexpected) behaviour of the tennis ball drag coefficient is explained in terms of a new flow model that includes the drag contribution of the 'fuzz' elements.

Keywords: aerodynamics, boundary layer, drag coefficient, flow separation, Magnus effect, tennis ball

Nomenclature

- d: Ball or sphere diameter
- D: Drag force on the sphere or ball
- k: Surface roughness height
- L: Lift force on the sphere or ball
- A: Projected area of the sphere or ball
- U: Ball or sphere velocity or wind tunnel velocity
- V: Equatorial velocity at the edge of the ball
- θ_s: Angle between the front stagnation point and the separation location

Correspondence address:
R. D. Mehta, Mail Stop 260–1, Fluid Mechanics Laboratory, NASA Ames Research Center, Moffett Field, California 94035–1000, USA. E-mail: rmehta@mail.arc.nasa.gov

ν: Kinematic viscosity of air
ρ: Density of air
C_D: Drag coefficient (= $D/\frac{1}{2}\rho U^2 A$)
C_L: Lift coefficient (= $L/\frac{1}{2}\rho U^2 A$)
Re: Reynolds number (= Ud/ν)
S: Spin parameter (= V/U)

Introduction

The game of tennis originated in France some time in the 12th century. It was originally played with the bare hand, but starting in the 16th century and continuing until the middle of the 18th century, rackets of various shapes and sizes were introduced. The game evolved into Real Tennis, which was played on a stone surface surrounded by four high walls and covered by a sloping roof. The oldest surviving Real Tennis court was originally built by King Henry VIII in about 1530 and it is located at Hampton Court Palace. The present day game of Lawn Tennis was derived from Real Tennis in 1873 by a Welsh army officer, Major Walter Wingfield.

It was in fact the flight of a tennis ball that first inspired scientists to think and write about sports ball aerodynamics. Newton (1672) had noted how the flight of a tennis ball was affected by spin and he wrote: 'I remembered that I had often seen a tennis ball ... describe such a curveline. For, a circular as well as a progressive motion being communicated to it by that stroke, its part on that side, where the motions conspire, must press and beat the contiguous air more violently than on the other, and there excite a reluctancy and reaction of the air proportionably greater'. Over two hundred years later, Rayleigh (1877) in a paper entitled: 'On the Irregular Flight of a Tennis Ball', commented that: '... a rapidly rotating ball moving through the air will often deviate considerably from the vertical plane'. He added the following interesting thoughts: '... if the ball rotate, the friction between the solid surface and the adjacent air will generate a sort of whirlpool of rotating air, whose effect may be to modify the force due to the stream'. Despite all this early attention, when the first review article on sports ball aerodynamics was published (Mehta 1985), no scientific studies on tennis balls could be identified and so tennis ball aerodynamics were not discussed.

The first published study of tennis ball aerodynamics was that due to Stepanek (1988) who measured the lift and drag coefficients on a spinning tennis ball simulating the topspin lob. The aerodynamic forces were determined by projecting spinning tennis balls into a wind tunnel test section. Empirical correlations for the lift and drag coefficients (C_L and C_D) were derived in terms of the spin parameter (S) only; it was concluded that a Reynolds number dependence could be neglected. Stepanek measured values of between 0.55 and 0.75 for C_D, and between 0.075 and 0.275 for C_L, depending on the spin parameter, which was varied between about 0.05 and 0.6. The extrapolated C_D for the nonspinning case was found to be about 0.51. Some work on the aeromechanical and aerodynamic behaviour of tennis balls was conducted at Cambridge University in the late 1990s (Brown & Cooke 2000; Cooke 2000). One of the more significant conclusions of these investigations was that the tennis ball would reach a quasi-steady aerodynamic state very soon after leaving the racket, in approximately 10 ball diameters, which is equivalent to only about 3% of its trajectory (Cooke 2000). So the initial transient stage, when the ball is still deformed and the flow around it is still developing, will not generally make a significant contribution to the overall flight path. Based on comparisons with Achenbach's (1974b) drag measurements on rough spheres, it was estimated that the critical Reynolds Number for a tennis ball would be about 85,000, based on a 'nap' or 'fuzz' height of about 1 mm. It was therefore deduced that for Reynolds Numbers normally encountered during a serve, $100\,000 < Re < 200\,000$ (corresponding to a serving velocity range of $26 < U < 46$ m s^{-1} or $57 < U < 104$ mph),

the ball would be in the supercritical regime giving a drag coefficient of about 0.3–0.4. However, some recent measurements on nonspinning tennis balls (discussed below) showed that the drag coefficient was higher and appeared to be independent of Reynolds Number.

Most of the recent research work on tennis ball aerodynamics was inspired by a decision made by the International Tennis Federation (ITF) to start field testing of a slightly larger 'oversized' tennis ball (roughly 6.5% larger diameter). This decision was instigated by a concern that the serving speed in (men's) tennis had increased to the point where the serve dominates the game. The fastest recorded serve was produced by Greg Ruzedski in March 1998 and it was measured at 66.6 m s^{-1} or 149 mph (Guinness 2000). The main evidence for the domination of the serve in men's tennis has been the increase in the number of sets decided by tie breaks at the major tournaments (Haake *et al.* 2000). This is particularly noticeable on the faster grass courts such as those used at Wimbledon.

Chadwick & Haake (2000a) obtained tennis ball C_D measurements using a force balance mounted in a wind tunnel. The initial measurements gave a C_D of about 0.52 for a standard tennis ball as well as the larger ball and it was found to be independent of Re over the range, $200\,000 < Re < 270\,000$. More recently, Chadwick & Haake (2000b) and Haake *et al.* (2000) reported that $C_D \cong 0.55$ over the same Re range for a standard tennis ball, a pressureless ball and a larger ball. The difference between the two reported C_D levels is attributed to the technique used to measure the ball diameter (Cooke 2000). Chadwick & Haake (2000a) used an outer (projected) diameter, which included the nap or fuzz height. Their results also showed that the tennis ball C_D could be increased (by raising the fuzz) or decreased (by shaving off the fuzz) by up to 10% (Chadwick & Haake 2000a; Chadwick & Haake 2000b; Haake *et al.* 2000).

The present project started as a collaborative effort between the National Aeronautics and Space Administration (NASA) and Cislunar Aerospace, Inc. to develop an Internet based educational programme designed to instruct students and educators on sports science (http://wings.avkids.com/Tennis). Using tennis as its theme, the materials provide an interactive study of the basic aerodynamics, physics, mathematics, motion capture and analysis techniques and biomechanics; some examples of these various aspects of the project are given in Pallis & Mehta (2000). The main objective of this particular part of the tennis project, which concentrated on tennis ball aerodynamics, was to understand the basic fluids principles of a tennis ball with emphasis on identifying the flow regimes and the parameters that affect the flight of the ball. A comparison and discussion of the aerodynamics of a variety of sports balls, including tennis balls, is given in a recent paper by Mehta & Pallis (2001).

Experimental apparatus and techniques

All the experiments on tennis ball aerodynamics reported here were conducted in wind tunnels in the Fluid Mechanics Laboratory at NASA Ames Research Center.

For the flow visualization studies, a 28-cm (11 inch) diameter 'model' tennis ball (Wilson Jumbo U.S. Open tennis ball) was used in a 1.2 × 0.8 m (48 × 32 inch) test section of an open-circuit wind tunnel. The larger model was used so that the test could be conducted at lower flow velocities, thus making it easier to visualize the flow patterns. Also, for a given spin parameter (S), a lower spin rate is required for the larger model, thus minimizing structural demands on the support mechanism. The testing procedure involves matching the Reynolds numbers and spin parameters commonly encountered on a tennis court. Therefore, for a given Re and S, the ball (or flow) velocity and the rotational velocity, can be lower if the ball diameter is increased. Although the fuzz and seam were not scaled accurately to the larger diameter of the ball, this was not considered to be critical to this qualitative flow visualization element of the study. The flow visualization technique consisted of injecting smoke into the flow (ahead of the ball) and then observing the flow over the ball by illuminating the smoke particles using a light sheet (Fig. 1).

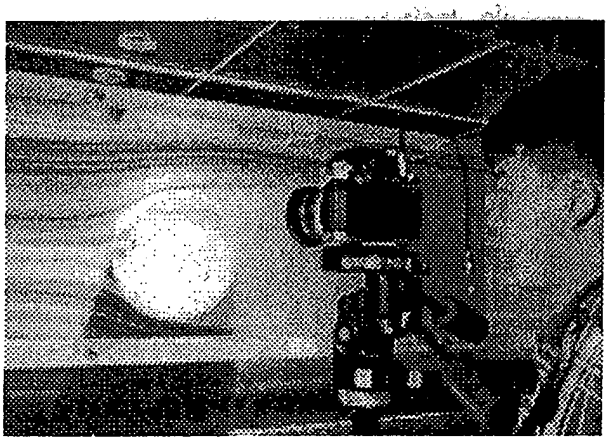

Figure 1 Wind tunnel set-up for smoke flow visualization studies over a 28-cm (11-inch) diameter tennis ball model. Flow in the wind tunnel is from left to right.

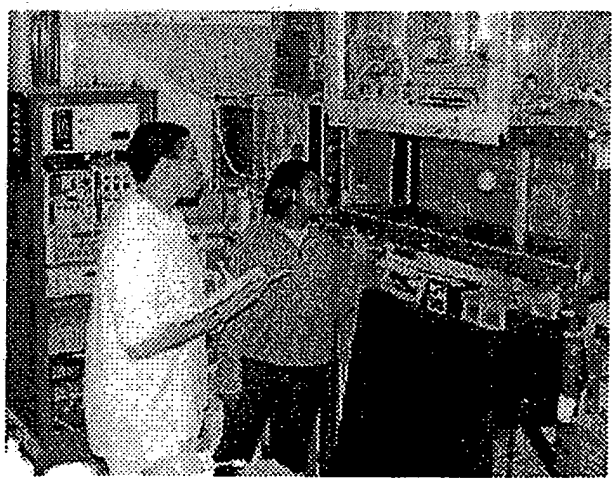

Figure 2 Wind tunnel set-up for tennis ball drag measurements. Flow in the wind tunnel is from left to right.

The ball was filled with rigid polyurethane foam, which preserved the ball's shape and provided a means to attach the ball to a support structure. The model was bonded to a 2.5-cm (1 inch) steel rod attached to a support outside the wind tunnel test section. A pulley/belt system connected to a small, variable-speed motor was mounted at the end of the steel rod, which allowed the ball to be spun. The flow visualization studies were conducted at wind tunnel flow velocities of 9–16 m s^{-1}; this corresponded to a *Re* range of 167 000–284 000 and standard-sized tennis ball ($d = 6.6$ cm) velocities of 39–66 m s^{-1} (87–148 mph). Spin rates of 1–4 revs s^{-1} were investigated on the 28-cm model, which corresponded to rates of 18–72 revs s^{-1} on a standard-sized ball.

A second series of wind tunnel tests were conducted to determine the drag coefficient of several types of tennis balls over a wide range of *Re*. A variety of tennis balls and spheres were tested including new and used standard-sized tennis balls, the recently introduced oversized tennis balls, a smooth Plexiglas sphere and a bald tennis ball (rubber core of a tennis ball without the outer fabric cover).

An open-circuit wind tunnel with a 0.38 × 0.38 m (15 × 15 inch) test section was used for these measurements (Fig. 2). A settling chamber, with honeycomb and eight screens followed by a 10 : 1 contraction, results in a high-quality test section flow with nonuniformity below 0.5%, angularity below 0.3° and a turbulence intensity level of 0.07%. Each tennis ball was filled with rigid polyurethane foam and mounted on a sting attached to a symmetric airfoil-shaped strut. This resulted in test section blockage of only about 2% (based on cross-sectional area) and so blockage corrections were not applied. The strut was attached to a reaction torque cell, which measured the drag force. To damp the higher-frequency vibrations from this assembly, the bottom of the strut had an extension attached to it, which protruded through the test section floor and was immersed in a small container of high-viscosity oil. The vibrations are mainly a result of unsteady forces induced by vortex shedding from the ball (Achenbach 1974a; Taneda 1978). The damping system enables the use of more reasonable averaging times for the data acquisition. The tare of the system was measured to account for the drag of the sting and strut assembly. In order to include additional effects caused by vortex shedding and turbulence in the ball wake, a tare ball was held in place through a separate mount from the side of the wind tunnel, but not touching the sting. The drag measurements were made over a wind tunnel flow velocity range of about 19–70 m s^{-1} (43–157 mph), which corresponds to a *Re* range of about 80 000–300 000. The ball diameter was measured using a pair of calipers; the caliper width was

adjusted until the ball slid through the opening without too much effort and an average diameter was determined from measurements across several axes through the ball.

The balls were obtained from several sources: the regular balls were purchased off the shelf, the prototype models of the new oversized balls were obtained from two different manufacturers through the United States Tennis Association (USTA); and a ball used at the 1997 US Open tournament.

Results and preliminary discussion

Flow Visualization Studies

The first tests were conducted with the 28-cm diameter tennis ball stationary (not spinning). The first observation at the lower test velocities was that the boundary layer over the top and bottom of the ball separated relatively early, near the apex at about 80–90 degrees from the front stagnation point (Fig. 3). This normally implies that the boundary layer is laminar (transition to a turbulent state has yet to occur). However, on increasing the wind tunnel velocity, even up to the maximum, resulting in $Re = 284\,000$ and standard-sized ball velocity of 66 m s^{-1} (148 mph), no significant changes were observed. This was somewhat surprising since, at some point, the assumed laminar boundary layer was expected to undergo transition, which would be evidenced by a sudden rearward movement of the separation point, thus leading to a smaller wake and less drag. So a new conclusion was reached which presumed that transition had already occurred and that a turbulent boundary layer separation was obtained over the whole *Re* range tested. Although the fabric cover was expected to affect the critical *Re* at which transition occurs, it seemed as though the roughness associated with the fuzz was a more effective boundary layer trip than had been anticipated. The fact that the boundary layer separation over the top and bottom of the nonspinning ball was symmetric leading to a horizontal wake was, of course, anticipated since a side force (upward or downward) is not expected in this case. In one series, the ball orientation was altered to check for seam effects, in particular to see if the seam could generate an asymmetric boundary layer separation, and hence side force, on the ball. However, the boundary layer separation remained symmetric and unaffected by the seam orientation, even when the seam was in the vicinity of the separation location. So the flow visualization data suggested that the seam probably does not play a critical role in determining the aerodynamics of a tennis ball. The seam orientation was also investigated during the drag measurement phase of the investigation, as discussed below.

In the second round of testing, spin was imparted to the ball by rotating the support rod. In Fig. 4, the ball is spun in a counter-clockwise direction to simulate a ball with topspin while in Fig. 5 the ball is spun in a clockwise direction, thus simulating underspin or backspin. In Figs 3 and 4, the wind tunnel flow speed was 9 m s^{-1} and the model was

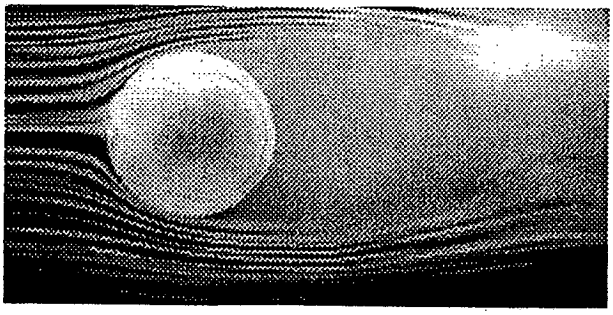

Figure 3 Flow visualization of 28 cm diameter tennis ball model with no spin ($Re = 167\,000$). Flow is from left to right.

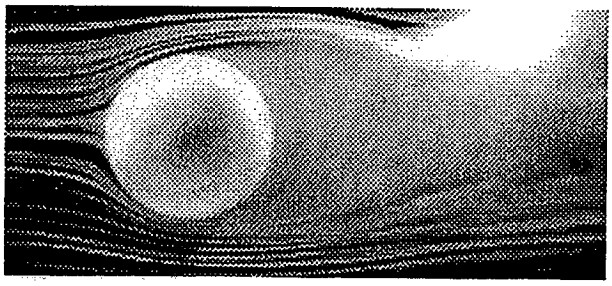

Figure 4 Flow visualization on ball with topspin (counter-clockwise rotation at 4 revs s^{-1}, $Re = 167\,000$). Flow is from left to right.

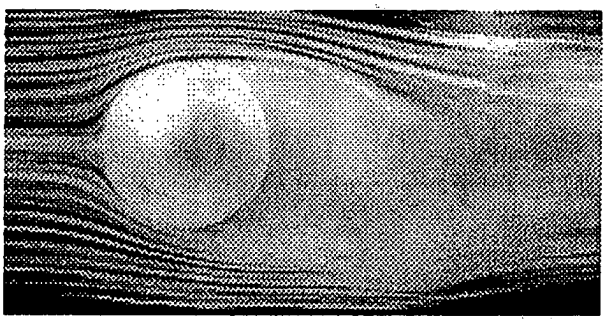

Figure 5 Flow visualization on ball with underspin (clockwise rotation at 4 revs s^{-1}, $Re = 167\,000$). Flow is from left to right.

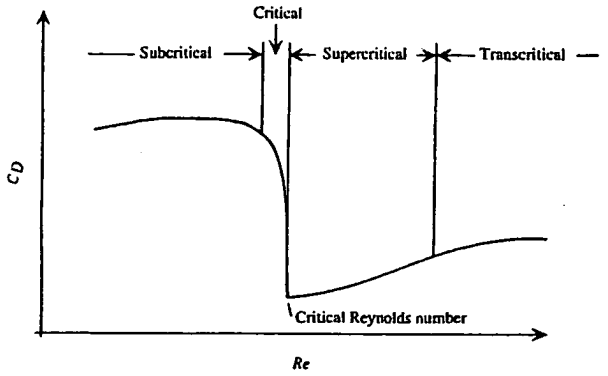

Figure 6 Flow regimes on a sphere (based on Achenbach 1972).

spun at 4 revs s^{-1}, which corresponds to a standard tennis ball velocity of 39 m s^{-1} (87 mph) and spin rate of 72 revs s^{-1} (4320 r.p.m.); this would represent a typical second serve in men's professional tennis. In Fig. 4, the boundary layer separates earlier at the top of the ball compared to the bottom. This results in an upward deflection of the wake behind the ball, and following Newton's 3rd Law of Motion, implies a downward (Magnus) force acting on it which would make it drop faster than a nonspinning ball. On the other hand, in Fig. 5 the wake is deflected downwards which means that the ball has an upward Magnus force acting on it that would make it travel further than a nonspinning ball. The fact that the Magnus force occurred in a direction that was expected (positive Magnus force) over the whole speed and spin ranges further suggested that transition had occurred and that the boundary layer over both sides (top and bottom) of the ball separated in a turbulent state. A negative Magnus force is generated when transition occurs on the advancing side, but the boundary layer on the retreating side still separates in a laminar state.

Drag Measurements

The flow over a sphere can be divided into four distinct regimes (Achenbach 1972). These regimes are illustrated in Fig. 6 in which the drag coefficient (C_D) is plotted against the Reynolds number (Re). In the subcritical regime, laminar boundary layer separation occurs at $\theta_s \cong 80°$ and the C_D is nearly independent of Re. In the critical regime, the C_D drops rapidly and reaches a minimum at the critical Re. The initial drop in C_D is due to the laminar boundary layer separation location moving downstream ($\theta_s \cong 95°$). At the critical Re, a separation bubble is established at this location whereby the laminar boundary layer separates, transition occurs in the free-shear layer and the layer reattaches to the sphere surface in a turbulent state. Achenbach (1972) proposed that the presence of a separation bubble was consistent with the relatively low value of the local minimum in the measured skin friction coefficient in this region. The turbulent boundary layer has higher momentum near the wall, compared to the laminar layer, and it is continually replenished by turbulent mixing and transport. It is therefore better able to withstand the adverse pressure gradient over the back part of the ball and separation is delayed to $\theta_s \cong 120°$. In the supercritical regime, transition occurs in the attached boundary layer and the C_D increases gradually as the transition and separation locations creep upstream with increasing Re. A limit is reached when the transition location moves all the way upstream, very close to the front stagnation point. The turbulent boundary layer development and separation is then determined solely by the sphere surface roughness and the C_D becomes independent of Re since the transition location cannot be further affected by increasing Re. Since the flow behaviour, in particular the boundary layer separation location, in the flow

visualization studies appeared to be independent of *Re*, the tennis ball was believed to be in this transcritical flow regime.

In order to verify the accuracy of the whole measurement system, the first test was conducted on a smooth Plexiglas sphere with about the same diameter ($d = 6.35$ cm) as a standard tennis ball. The results (Fig. 7) compare very well with the classic data of Achenbach (1972, 1974b). A C_D of about 0.5 with a slight increase with *Re* initially, followed by a decrease at the higher *Re* as boundary layer transition is about to occur, are all evident in these measurements. Transition, evidenced by a sudden drop in C_D, occurs at a *Re* of about 400 000 for a smooth sphere, as seen in this figure. Premature transition can occur (at a lower *Re*) if the wind tunnel flow quality is inadequate (high turbulence levels) or if the model vibrates significantly; the fact that it does not occur here is again evidence of a suitable experimental set up. Achenbach's data for rough spheres show that the critical *Re*, and the amount by which the C_D drops, both decrease with increasing surface roughness. At the same time, the (constant) C_D level in the transcritical region increases with roughness for the roughness levels shown.

The new (unused) tennis ball C_D data are presented in Fig. 8, together with the smooth sphere data and those for a 'bald' ball (the inner rubber core of a tennis ball) over a *Re* range of about 80 000–300 000. In Fig. 8, the ball velocity quoted along the upper horizontal axis is that for a

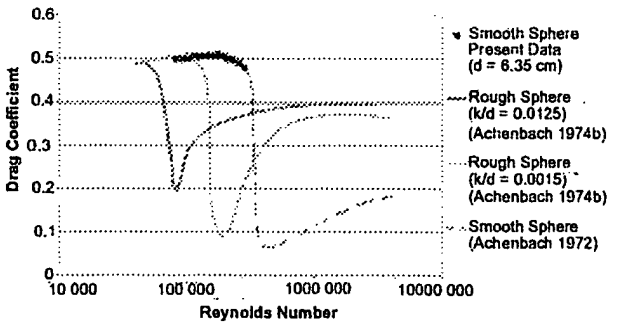

Figure 7 Drag Coefficient vs. Reynolds Number for smooth and rough spheres.

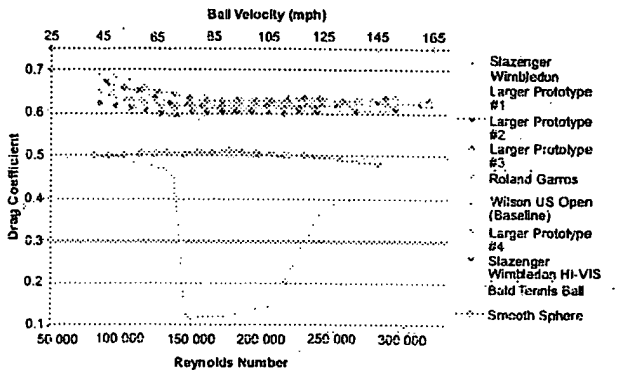

Figure 8 Drag Coefficient vs. Reynolds Number for new tennis balls.

standard-sized tennis ball ($d = 6.6$ cm). The bald ball surface was quite smooth except for a small ridge along the equator where the two halves of the ball are joined together. This ball was mounted with the ridge perpendicular to the flow. Transition occurs at a *Re* of about 140 000, considerably lower than that for a smooth sphere since the ridge acts as a boundary layer trip. The C_D in the supercritical regime remains more or less constant up to about $Re = 200\,000$. In this *Re* range, transition is still triggered by the ridge on the ball. However, beyond $Re = 200\,000$ the C_D starts to increase again as transition moves upstream of the ridge and the separation also moves towards the front of the ball. The rise in C_D is rather abrupt because the turbulent boundary layer is thickened by the ridge, thus making it more susceptible to separation. Beyond $Re \cong 280\,000$, the ball would be in the transcritical regime and the C_D would be expected to level off at a constant value, perhaps slightly above 0.4, similar to Achenbach's (1974b) observations for rough spheres.

The results for the new (unused) tennis balls show an approximately constant C_D of about 0.6–0.65 at the higher *Re* (>150 000). In the lower *Re* range (85 000 < *Re* < 150 000), it was rather surprising to see higher values of C_D, achieving values of up to 0.7. A Reynolds number dependence also develops in this range with the C_D decreasing with increasing *Re*. These data include measurements for some of the new oversized tennis balls. At the higher

Re, the tennis ball is clearly in the transcritical regime, only at relatively low *Re* compared to the smooth and rough sphere data of Achenbach (1972, 1974b). So it appears as though the fabric cover on the ball is very effective at causing early transition and also in thickening the turbulent boundary layer. The C_D data for each ball presented in this figure were averaged over several (between 3 and 10) separate runs. The run to run repeatability was better on some balls than others. For example, the C_D repeatability on the baseline Wilson US Open ball was about ±0.01. Although some of the variation was no doubt due to the unsteady nature of the flow field, because of vortex shedding in the wake, this ball to ball difference was somewhat of a mystery at first; this aspect of the results is further discussed below in the next section.

In one phase of the drag measurement testing, the effects of tennis ball seam orientation were investigated to verify the observations and conclusions drawn from the flow visualization studies. For most of the drag measurement tests, the tennis ball was mounted with the manufacturer's marking in the horizontal plane and facing the oncoming flow (similar orientation to that shown in Fig. 1). Two additional Wilson US Open balls were also tested with the marking facing to the side on one ball and facing downstream on the other. The drag measurements repeated to within the ±0.01 tolerance quoted above, thus further indicating a lack of seam effects. Although ball seam orientation can affect the flight and trajectory of other sports balls, these effects were not observed on the tennis ball. Unlike cricket balls and baseballs (Mehta 1985), the seam on a tennis ball is indented and the cover surface is very rough, thus obscuring or overwhelming any seam effects.

For $Re > 150\,000$, the data in the transcritical regime for each ball are averaged to give a single value for the C_D and these data are presented in Fig. 9. The lowest C_D is that for the Slazenger Wimbledon Hi-Vis at just above 0.6 while the highest C_D is that for one of the prototype oversized balls at just above 0.63, with all the other balls tested scattered in between. So basically the C_D for all the new balls tested, including the larger balls, falls

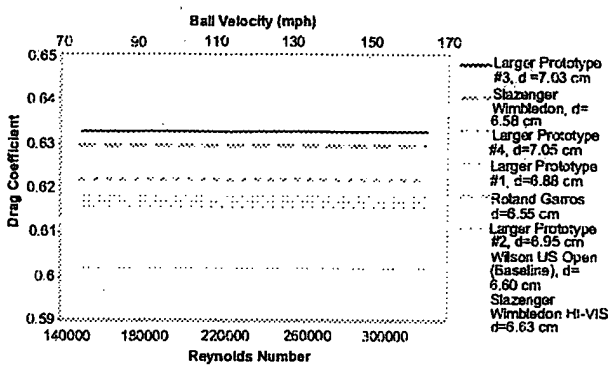

Figure 9 Drag Coefficient vs. Reynolds Number for new tennis balls in transcritical regime.

within about 5% of each other. Furthermore, given the repeatability quoted above, not too much should be made of the differences in C_D between the balls tested. The important point to note is that the C_D values for the larger balls are comparable to those for the regular balls. Of course, this is not all that surprising since a simple scaling of the size should not affect the C_D, as long as other parameters, such as the surface characteristics (e.g. details of the fuzz), are not altered significantly. As a result, the drag on the oversized ball will increase by an amount proportional to the cross-sectional area, and the desired effect of increasing the flight time for a given serve velocity will be attained.

Further Discussion

Right from the time the very first flow visualization tests were conducted, the indications were that the fabric cover on the tennis ball was very effective at triggering relatively early transition of the laminar boundary layer and also at rapid thickening of the turbulent boundary layer beyond transition. The fact that the flow pattern, in particular the separation location, was not affected by increasing *Re*, was the first indication that the ball was in the transcritical regime with turbulent boundary layer separation. In the transcritical regime, boundary layer transition occurs right next to the stagnation point and so a limit is reached whereby the transition and separation points cannot move further upstream with increasing *Re*.

The main point of concern was the relatively high values of the measured C_D for the tennis balls. The turbulent boundary layer separation location for the tennis ball appeared to be comparable to that seen for laminar separation at relatively low *Re*. Now, the total drag on a bluff body, such as a sphere or tennis ball, consists mainly of pressure drag (due to the pressure difference between the front and back of the ball) and a very small contribution due to viscous or skin friction drag (due to the no slip condition). Achenbach (1972) showed that the viscous drag for a smooth sphere approaching the transcritical regime was about 2% of the total drag. So the bulk of the total drag is accounted for by pressure drag, which in turn is determined solely by the boundary layer separation location on the ball. Since the separation location for the tennis ball is comparable to that for laminar separation at low *Re*, one would expect the C_D for the tennis ball to be around 0.5. However, the present measurements give a C_D of about 0.62 for the tested (new or unused) tennis balls. The previously measured C_D values of 0.51 (Stepanek 1988) and 0.55 (Chadwick & Haake, 2000b; Haake *et al.* 2000) are also above the 0.5 level. Some of the difference in the measured C_D values between the different investigations can be attributed to the different techniques used to measure the ball diameter. The main task in the present investigation was to determine why the tennis ball C_D was higher than 0.5 and where the additional drag contribution was coming from.

As explained above, in the supercritical regime, once transition has occurred, the transition and separation locations start to creep upstream and so the C_D starts to increase. At some point, the transition location moves all the way up to the stagnation location and the separation location is then totally determined by the development of the turbulent boundary layer. With increasing roughness, the boundary layer growth rate is increased, thus resulting in earlier separation and higher C_D. The constant level achieved by the C_D in the transcritical regime is also expected to increase with increasing roughness, as evidenced in Achenbach's (1974b) measurements (data for two roughness levels are shown in Fig. 7). However, Achenbach's data show an upper limit of $C_D \cong 0.4$ on spheres with increasing roughness (Figs 2 and 4 in Achenbach 1974b show this limit for a k/d range of 0.0025–0.0125). The measured separation location for this value of C_D was about $\theta_s \cong 100°$. This is still in the region of the adverse pressure gradient and so one would expect the boundary layer separation location to continue moving upstream with increasing surface roughness. However, the point to note is that while the boundary layer growth (rate of thickening) increases with increasing roughness, so does its skin friction coefficient and the behaviour of the separation location is then determined by the behaviour of these competing effects. The increasing skin friction coefficient makes the boundary layer more resilient to separation, thus opposing the tendency of a boundary layer to separate as it thickens. So it is entirely possible that for certain types of roughness, such as the round glass beads investigated by Achenbach for example, a limit is reached for the C_D level in the transcritical regime because the effects of the boundary layer thickening are offset by those due to the increasing skin friction coefficient.

In principle though, there is no reason why the separation location cannot continue to creep forward for other types of roughness elements, which may be more effective at thickening the boundary layer than increasing the skin friction coefficient. It is proposed here that the absolute limit for the turbulent boundary layer separation location in the transcritical regime is the same as that for laminar boundary layer separation in the subcritical regime ($\theta_s \cong 80°$). Laminar boundary layer separation occurs upstream of the sphere apex because of the presence of an adverse pressure gradient in this region (see Fig. 7b in Achenbach 1972). The adverse pressure gradient is generated in this region due to an upstream influence of the separated near wake. One effect which occurs is that initially, when the flow is first turned on, the laminar boundary layer separates at the apex and immediately a pressure minimum is generated upstream of it due to streamline curvature effects, much in the same way as that generated near the exit region of a

contraction (Bell & Mehta 1988). Once this adverse pressure gradient is generated, the laminar boundary layer separation will tend to move to that location. This is probably the most upstream location that the adverse pressure gradient can move up to. Assuming that a very thick (weak) turbulent boundary layer can become as prone to separation as a laminar layer, then it will separate as soon as it encounters an adverse pressure gradient (at about $\theta_s \cong 80°$), just like the laminar layer. So if the location for turbulent separation in the transcritical regime is similar to that of laminar separation in the subcritical regime, then the pressure drag should also be comparable, thus giving a total drag of $C_D \cong 0.5$.

On examining the tennis ball, the relatively rough surface on the outer cover is readily apparent. The roughness actually results from the junctions of the fuzz elements, where they are embedded within the fabric covering on the ball. However, in addition, the fuzz elements have a finite thickness and length and this forms an additional porous coating on the ball through which air can still flow. So the tennis ball can be thought of as a very rough sphere with a porous coating. Subsequently, each fuzz element will also experience pressure drag and when this is summed up for all the fuzz elements on the ball's surface, one obtains the additional drag contribution and this is herein termed the 'fuzz drag'. So the present data suggest that the contribution of the fuzz drag to the total drag on the tennis ball is between 20% and 40%, depending on the *Re*.

The other trend in the tennis ball C_D measurements, which was initially puzzling, was the higher values of C_D at the lower *Re* (Fig. 8). At first it was tempting to discard the trend by attributing it to experimental error since both, the tunnel reference pressure and drag force (drag count), become harder to measure accurately as the wind tunnel flow speed is reduced (the percentage error increases as the mean values are lower). However, in this particular case, the smooth sphere data in the same *Re* range look consistent and agree very well with previous measurements, as shown in Fig. 7. Moreover, compared to the smooth sphere, the overall drag-count error for the tennis balls would be lower since the drag is higher. All past measurements for rough spheres had shown that the approach to a constant C_D level in the transcritical regime was from below, from a lower critical value (C_D increases with *Re* in the supercritical and early part of the transcritical regimes until a constant level is attained). Once again the fuzz elements and their behaviour with varying *Re* were identified as the only likely causes for the observed effect.

The first effect, which is perhaps not too surprising, is the change in orientation of some of the filaments. As the flow velocity is increased, many of the filaments that are initially standing almost perpendicular to the ball's surface are forced to lay down due to aerodynamic drag effects. Note how in Fig. 10, the fuzz filaments, particularly over the front face of the ball, and up to the apex region, tend to lay down at the higher flow speed. Hence the contribution of the fuzz drag is reduced at the higher flow speeds or *Re*. Also, the fuzz element *Re* (based on filament diameter) is estimated to be of order 20, and this puts it in a range where the C_D (for a circular cylinder) is much higher ($C_D \cong 3$) and a strong function of the *Re*, with the C_D decreasing with increasing *Re* (see Fig. 10.12 in Smits 2000). So the higher C_D level at the lower ball *Re* investigated, is attributed to the combined effect of fuzz filament orientation and *Re* effects on the individual filaments.

All the new (unused) tennis balls exhibited this trend of higher C_D at the lower tested *Re* (Fig. 8),

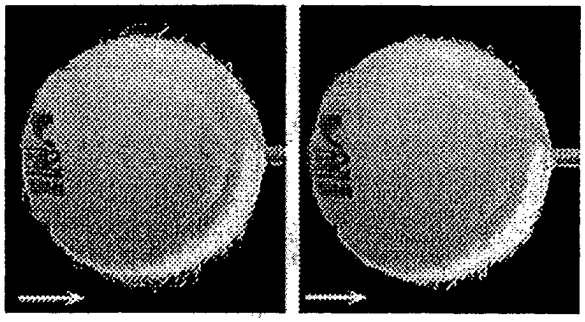

Figure 10 Effect of flow velocity on fuzz element orientation. Left-hand photo, $U = 20$ m s^{-1} (45 mph, $Re = 100\,000$). Right-hand photo, $U = 60$ m s^{-1} (135 mph, $Re = 260\,000$). Flow is from left to right.

but not to the same extent. The data for the two balls, which showed the maximum and minimum rise in C_D at the lower Re, are shown in Fig. 11. Ironically, they are both Slazenger Wimbledon balls, but it was noted while testing that the fuzz filaments on the 'Hi-Vis' ball were not affected as much (did not lay down as much) at the higher Re as the other Slazenger ball. Also, the drag measurement repeatability on the Hi-Vis ball was much better than on any other ball. Apparently, the only difference between the two Slazenger balls was in the fabric dyeing process and it is possible that this resulted in stiffer fuzz filaments on the Hi-Vis ball. The stiffer filaments led to a lower dependence on Re, since the filament orientation is not affected as much by Re, and also to better repeatability since the filaments are affected less by operational procedures, such as handling and storing.

The critical role of the fuzz in determining the tennis ball drag was borne out most succinctly in the results for the used balls (Fig. 12). One of the balls was used in the 1997 US Open for nine games and the other used balls were played with by recreational players for the noted number of games, using only two balls at a time. The baseline data for the new Wilson US Open ball are also shown for reference. The 1997 US Open ball seems to indicate a supercritical behaviour with the critical Re of about 100 000 and then a gradual approach towards the transcritical regime. For the balls used by the recreational players, after three games the C_D behaviour is comparable to that of the new ball.

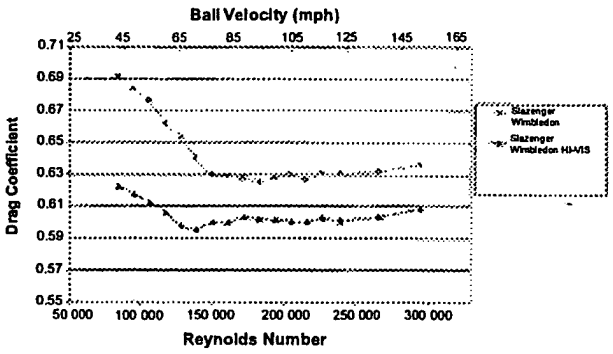

Figure 11 Drag Coefficient vs. Reynolds Number for new Slazenger balls.

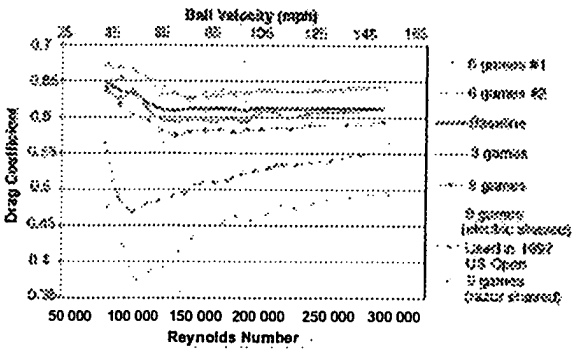

Figure 12 Drag Coefficient vs. Reynolds Number for used Wilson US Open balls.

However, after six games the C_D is clearly higher and to confirm this increase, both the used balls were tested and they show a very consistent trend with excellent repeatability. This initial increase in C_D is supposedly known to tennis players who often refer to the cover as having 'fluffed-up' (raised fuzz), which would obviously account for the higher drag. The fluffing-up was not apparent when these two balls were examined visually, but the present C_D measurements strongly suggest that the fabric texture, perhaps the internal fuzz structure, must have been affected. The nine game ball clearly exhibited a worn cover (shorter fuzz elements) and so it was not too surprising to see a lower measured C_D. The fact that a fluffed-up cover results in an increased C_D and a worn cover in a reduced C_D was not too surprising since the effect had been previously observed by Chadwick (Chadwick & Haake 2000a; Chadwick & Haake 2000b; Haake *et al.* 2000).

The C_D for the nine game ball was still a lot higher and the behaviour with Re quite different compared to that of the 1997 US Open ball. This is not too surprising since the recreational players are obviously not expected to hit the ball as hard or have as many rallies as the professionals at the US Open. In order to try and replicate the 1997 US Open ball data, it was decided to accelerate the wear on the nine game ball by shaving-off the remaining fuzz. An electric razor was used at first, which removed some of the fuzz and the C_D in the transcritical regime was reduced as a result.

However, the electric razor also tended to fluff-up the cover, since the filaments often caught in the razor when it was lifted off the surface, and the higher rise in C_D at the lower Re is attributed to this effect. As a final effort, a razor blade was used to shave-off as much of the fuzz as possible. Note that even this level of shaving does not remove the fuzz and associated roughness completely; the surface is similar to that on a man's face with about a two day stubble. This ball clearly shows a C_D behaviour that is comparable to that of the 1997 US Open ball, with about the same critical Re and supercritical behaviour. However, the C_D levels are lower throughout the Re range and this is because there is no contribution due to the fuzz drag. The effective surface roughness on this shaved ball and the 1997 US Open ball is probably comparable, which explains the similar value of the critical Re. Also, as is hypothesized above, the maximum C_D in the transcritical regime on a very rough sphere, with no contribution from the roughness element drag (fuzz drag), should be 0.5 and that is exactly the level this shaved ball C_D seems to be asymptoting towards.

Conclusions

The fact that the flow over a new tennis ball was essentially in the transcritical regime, where the separation location does not move significantly with Re, was clearly suggested by the flow visualization results. This in turn implies that the C_D is independent of Re since the total drag on a bluff body, such as a round ball, is almost totally accounted for by the pressure drag and this was confirmed by the drag measurements. The fabric cover on a tennis ball is very effective at causing very early transition of the laminar boundary layer and rapid thickening of the turbulent boundary layer. This results in the separation location moving up to the apex region, comparable to that for laminar boundary layer separation at subcritical Re. In this case, the total drag for the tennis ball would be expected to be about the same as that for a ball in the subcritical regime, thus giving $C_D \cong 0.5$. However, all the previous and present measurements indicate that the C_D for a new (unused) tennis ball is higher than 0.5, the exact value depending to some extent on the measurement and definition of the ball diameter. C_D values of between 0.6 and 0.7 were measured in the present investigation for new tennis balls in the Re range, $80\,000 < Re < 300\,000$. So there must be another drag contribution and it is proposed here that the additional drag is due to pressure drag on the individual fuzz elements. This additional contribution is herein defined as the 'fuzz drag' and the present measurements show that, depending on the ball Re, it can account for 20% to 40% of the total drag on new tennis balls. The higher levels of C_D at the lower Re ($80\,000 < Re < 150\,000$) are attributed to the dependence of fuzz element orientation on flow (or ball) velocity and the stronger dependence of C_D on Re at the very low fuzz element Re. The recently approved oversized tennis ball C_D is comparable to that for the standard-sized balls. However, the drag on the oversized balls is higher by virtue of the larger cross-sectional area and so the desired effect of 'slowing down the game' (increased tennis ball flight time) will be achieved.

The most revealing results from this investigation are those for the used balls. The C_D increases at first, presumably due to the ball fuzz 'fluffing-up', but it decreases with further use as the cover becomes worn and the fuzz starts coming off. In addition, the C_D of the tennis ball with a worn cover becomes a function of Re and the critical Re is identifiable. It is interesting to note that a ball used in a major tournament (1997 US Open) can achieve this state of lower C_D, which should make it more attractive for the faster servers in tennis. Of course, tennis players are also concerned about other attributes of the ball, such as 'liveliness' and 'controllability' and they therefore generally prefer to serve with new balls. For the ball with the razor-shaved fuzz, the critical Re is about 100 000 and the maximum C_D level in the transcritical regime approaches 0.5, as predicted by the present analysis. In view of the present findings, it is particularly intriguing to note that the current rules of tennis do not stipulate any technical specifications regarding the outer covering on a tennis ball. The ITF rule

simply states: 'The ball shall have a uniform outer surface consisting of a fabric cover and shall be white or yellow in colour'.

Acknowledgments

This work was supported through several agreements between NASA and Cislunar Aerospace, Inc. (NCC2-9014, NCC2-9010 and SAA2-400190). The authors wish to thank: the United States Tennis Association (USTA), Wilson Racquet, and Head/ Penn Racquet Sports for the oversized tennis balls; Greg Zilliac, David Yaste, Kent Shiffer and Kurt Long from NASA Ames and Jim Pallis and Kevin Okamoto from Cislunar Aerospace, Inc. for their assistance during the wind tunnel tests and summer students, Chris Ford and DaJuanicia Holmes for conducting the drag measurement experiments. We are also grateful to David Driver (NASA Ames) for many useful discussions, to J.T. Heineck for help with the graphics and to several of our colleagues for reviewing a draft of this paper.

References

Achenbach, E. (1972) Experiments on the flow past spheres at very high Reynolds number. *Journal of Fluid Mechanics*, **54**, 565–575.

Achenbach, E. (1974a) Vortex shedding from spheres. *Journal of Fluid Mechanics*, **62**, 209–221.

Achenbach, E. (1974b) The effects of surface roughness and tunnel blockage on the flow past spheres. *Journal of Fluid Mechanics*, **65**, 113–125.

Bell, J.H. & Mehta, R.D. (1988) Contraction design for small low-speed wind tunnels. NASA-CR 177488.

Brown, T.M.C. & Cooke, A.J. (2000) Aeromechanical and aerodynamic behavior of tennis balls. *Tennis Science and Technology* (Haake, S.J. & Coe, A., eds.) Proceedings of the 1st International Conference on Tennis Science and Technology. Blackwell Science, Oxford, UK, pp. 145–153.

Chadwick, S.G. & Haake, S.J. (2000a) The drag coeffcient of tennis balls. *The Engineering of Sport. Research*, Development and Innovation (Subic, A.J. & Haake, S.J., eds.) Proceedings of the 3rd International Conference on the Engineering of Sport. Blackwell Science, Oxford, UK, pp. 169–176.

Chadwick, S.G. & Haake, S.J. (2000b) Methods to determine the aerodynamic forces acting on tennis balls in flight. *Tennis Science and Technology* (Haake, S.J. & Coe, A., eds.) Proceedings of the 1st International Conference on Tennis Science and Technology. Blackwell Science, Oxford, UK, pp. 127–134.

Cooke, A.J. (2000) An overview of tennis ball aerodynamics. *Sports Engineering*, **3** (2), 123–129.

Guinness (2000) *Guinness World Records*, Millennium Edition. Guinness World Records Ltd, Bantam. London, UK.

Haake, S.J. *et al.* (2000) Engineering tennis – slowing the game down. *Sports Engineering*, 3 (2), 131–143.

Mehta, R.D. (1985) Aerodynamics of Sports Balls. *Annual Review* of Fluid Mechanics, **17**, 151–189.

Mehta, R.D. & Pallis, J.M. (2001) Sports ball aerodynamics: effects of velocity, spin and surface roughness. *Materials and Science in Sports Conference*, Coronado, California, April 22–25.

Newton, I. (1672) New theory of light and colours. *Philosophical Transactions of the Royal Society London*, **1**, 678–688.

Pallis, J.M. & Mehta, R.D. (2000) Tennis science collaboration between NASA and Cislunar Aerospace. *Tennis Science and Technology* (Haake, S.J. & Coe, A, eds.) Proceedings of the 1st International Conference on Tennis Science and Technology. Blackwell Science, Oxford, UK, pp. 135–144.

Rayleigh, Lord (1877) On the irregular flight of a tennis ball. *Messenger of Mathematics*, **7**, 14–16.

Smits, A.J. (2000) *A Physical Introduction to Fluid Mechanics*. John Wiley & Sons, New York.

Stepanek, A. (1988) The aerodynamics of tennis balls – the topspin lob. *American Journal of Physics*, **56**, 138–141.

Taneda, S. (1978) Visual observations of the flow past a sphere at Reynolds numbers between 10^4 and 10^6. *Journal of Fluid Mechanics*, **85**, 187–192.

Evidence Appendix D

***Golf Ball Aerodynamics*, by P.W. Bearman and J.K. Harvey, Aeronautical Quarterly, 1976, Volume 27, Pages 112-122**

This reference was originally entered in the record by the Primary Examiner in an Office Action mailed July 28, 2005.

Golf Ball Aerodynamics

P W BEARMAN AND J K HARVEY

(Imperial College of Science and Technology)

Summary: A wind tunnel technique has been developed to measure the aerodynamic forces acting on golf balls over a wide range of Reynolds number and spin rate. Balls with round dimples and hexagonal dimples have been investigated. The dimples are found to induce a critical Reynolds number behaviour at a lower value of Reynolds number than that experienced by a smooth sphere and beyond this point, unlike the behaviour of a sand-roughened sphere, there is little dependence of the forces on further increases in Reynolds number. A hexagonally-dimpled ball has a higher lift coefficient and a slightly lower drag coefficient than a conventional round-dimpled ball. Trajectories are calculated using the aerodynamic data and the ranges are compared with data obtained from a driving machine on a golf course.

1. Introduction

Golf, in common with many other games, is strongly influenced by the aerodynamic forces that act on a sphere. After the introduction of the gutta-percha ball in 1845, golfers discovered that it flew farther and better when scored or marked. Thus started the introduction of numerous cover designs chosen more or less by intuition. Among those tried included the "bramble ball" with a raised pattern, which unfortunately tended to accumulate mud, and covers with rectangular and square depressions. By 1930 the round dimple had almost completely taken over and became accepted as the standard design for golf balls. These "conventional" golf balls have either 330 or 336 round dimples placed in regular rows.

The trajectory of a golf ball is determined by the gravitational and aerodynamic forces acting on it during its flight. In addition to the drag, a lift force is generated by the back spin imparted to the ball by the angled face of the club. Initial rotational speeds of between 2000 and 4000 rpm have been measured for typical drive shots. The effect of the spin is to delay separation of the flow from the upper part of the surface and to advance it on the lower. The aerodynamic lift L and drag D acting on a spinning sphere depend on the velocity through the air U, the fluid density ρ and the viscosity μ. In addition they will depend on the diameter d and the rotational speed N, measured in revolutions per minute. It has been found convenient to express the spin in terms of the peripheral or equatorial speed v, where $v = \pi Nd/60$. Therefore we can write

$$L \text{ and } D = f(\rho, \mu, U, d, v).$$

From the rules of dimensional analysis, this equation becomes

$$C_L \text{ and } C_D = f\left(\frac{\rho U d}{\mu}, \frac{v}{U}\right),$$

where $\rho Ud/\mu$ is the Reynolds number Re and the velocity ratio v/U will be termed the spin parameter.

$$C_L = \frac{L}{\frac{1}{2}\rho U^2 S} \quad \text{and} \quad C_D = \frac{D}{\frac{1}{2}\rho U^2 S}$$

where $S = \pi d^2/4$, the projected area of the sphere. During a typical drive both the Reynolds number and the spin parameter will change and it is expected that the lift and drag coefficients will also vary. The spin parameter will be about 0.1 if the initial rpm of the ball is around 3500. During the flight the velocity of the ball will fall, thus reducing the Reynolds number, and, although there will be some decay of the spin, the drop in velocity will cause the spin parameter to increase.

Received January 1976

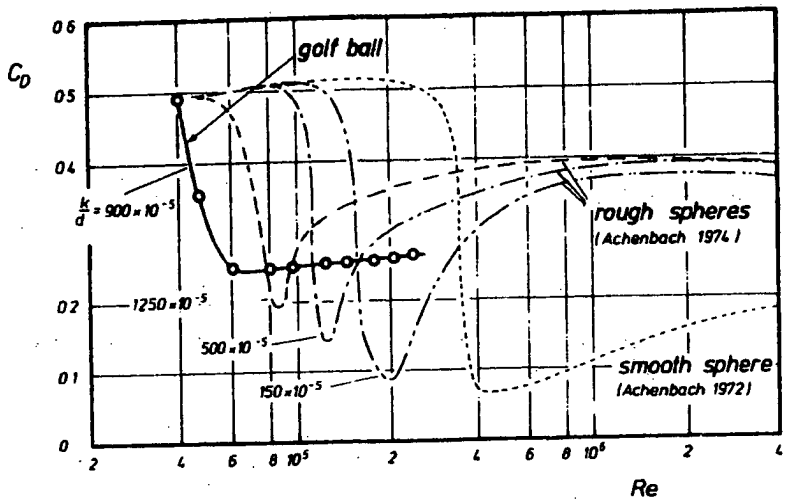

Figure 1 Variation of golf ball and sphere drag

The British golf ball has a diameter of 1.62 in (41.1 mm) and, assuming a speed of 75 m/s off the tee, the initial Reynolds number based on ball diameter is about 2.1×10^5. Figure 1, taken from Achenbach[1], clearly shows that a smooth sphere at this Reynolds number is in the high drag sub-critical flow regime where the boundary layer remains laminar up to separation. The addition of surface roughness, in the form of spherical grains, reduces the critical Reynolds number and, apart from the sphere with finest roughness, the drag coefficient quickly recovers, with increasing Reynolds number, to a value of about 0.4. This helps to explain why a dimpled golf ball can be driven further than a smooth one, but dimples are a very gross roughness and it is doubtful whether they can be compared directly with sand-roughened spheres.

Data on the aerodynamic forces experienced by spheres rotating about an axis normal to the flight direction are sparse. Figure 2 shows wind-tunnel measurements of Maccoll[2] and Davies[3]. C_D and C_L are plotted against the spin parameter v/U for a Reynolds number of about 10^5. Cases 1 and 2 are for a smooth sphere, whereas case 3 gives forces for a conventionally-dimpled golf ball. The accuracy of both sets of data is open to question. Maccoll supported his sphere on a spindle which had a diameter equal to about 15 per cent of the sphere diameter. Davies used a device which spun the ball up between a pair of rotating cups. The cups were parted, releasing the ball into the air stream. By noting the distance travelled by the sphere before it struck the floor of the tunnel, the aerodynamic forces could be deduced. A limitation of Davies's work was that the Reynolds number of his golf ball measurements was 9.4×10^4, i e somewhat less than the value expected of a golf ball leaving the tee. Some values of drag coefficient are presented by Williams[4], but these were deduced from range data assuming that both lift and spin are unimportant.

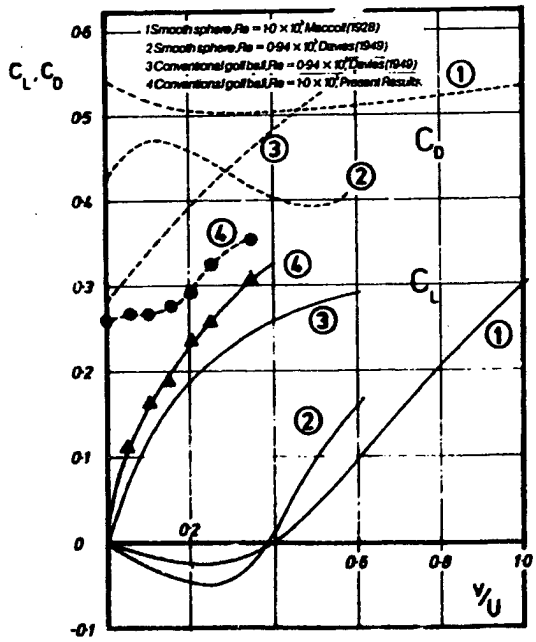

Figure 2 Lift and drag coefficients of rotating spheres versus rotational speed

The main aim of the present investigation was to measure the lift and drag forces acting on a golf ball in a wind tunnel and to use these data to predict golf ball trajectories. The ranges from these predicted trajectories can then be compared with actual ranges measured under controlled conditions. A further aim was to examine the effect on the aerodynamic forces, and hence the range, of changing the dimple shape. The forces on a conventionally-dimpled golf ball were compared with those on a ball having a dimple configuration similar to that on a Uniroyal Plus 6. The Plus 6 has 240 hexagonal dimples and 12 pentagonal dimples arranged in a triangulate pattern. The manufacturers claim that in most circumstances the Plus 6, hereafter called the hexagonally-dimpled ball, will carry farther than a conventional ball when given the same initial speed, spin and launch angle.

Notation

L	lift
D	drag
C_L	lift coefficient
C_D	drag coefficient
ρ	fluid density
μ	fluid viscosity
N	rotational speed
U	velocity through the air
d	diameter
v	peripheral velocity (spin), $=\pi Nd/60$
Re	Reynolds number, $=\rho Ud/\mu$
S	projected area of ball, $=\pi d^2/4$
k	average diameter of sand grains

2. Wind-Tunnel Experiments

2.1 EXPERIMENTAL ARRANGEMENT

The wind-tunnel measurements were made in the Imperial College, Department of Aeronautics 5 ft x 4 ft (1.524 m x 1.219 m) wind tunnel. This is of the closed return type and has a turbulence level of about 0.2 per cent. The maximum speed of the tunnel is around 45 m/s and therefore, in order to simulate the correct Reynolds number, it was necessary to use models of golf balls 2½ times full scale. The tunnel was operated up to speeds of about 37 m/s. This simulates flow on a golf ball at a speed of 92.5 m/s.

Three wind-tunnel models were made: a conventionally-dimpled ball, a hexagonally-dimpled ball and a smooth sphere. Various authors have pointed out the difficulty of accurately measuring the forces on spheres, owing to support interference. Since reliable data exist on the drag of a non-rotating smooth sphere, the results for our smooth sphere could be used to assess the degree of interference caused by the support system. The models were constructed as hollow shells moulded in glass reinforced plastic. Each shell was split in two to accommodate a motor and bearing assembly on which the ball revolved. These details are shown in Figure 3. Various support systems were tried and the one finally adopted was to suspend the ball from a wire of 0.50 mm diameter. A second wire of 0.20 mm diameter was attached to the underside of the ball, passing through the wind-tunnel floor and carrying a weight to keep the spin axis vertical. The diameter of the largest wire was only ½ per cent of the diameter of the golf ball model. The two wires also served to supply a voltage to the motor inside the ball.

The upper support wire was attached to a strain-gauged arm which measured the lift force on the ball (with the vertical spin axis this was in fact a side force). The strain-gauged arm was in turn mounted on a rigid support attached to the wind-tunnel three-component balance. The wind-tunnel balance was used to measure the drag. The strain-gauged arm and the rigid support were shielded from the air stream by a streamlined fairing. The drag of the exposed wires was subtracted from the total measured drag.

The rotational speed of the ball was measured by using a stroboscope, which was regularly calibrated during the experiments. Where air speeds and rpm are quoted in the paper, these have been scaled to the appropriate values for a golf ball of 41.1 mm (1.62 in) diameter.

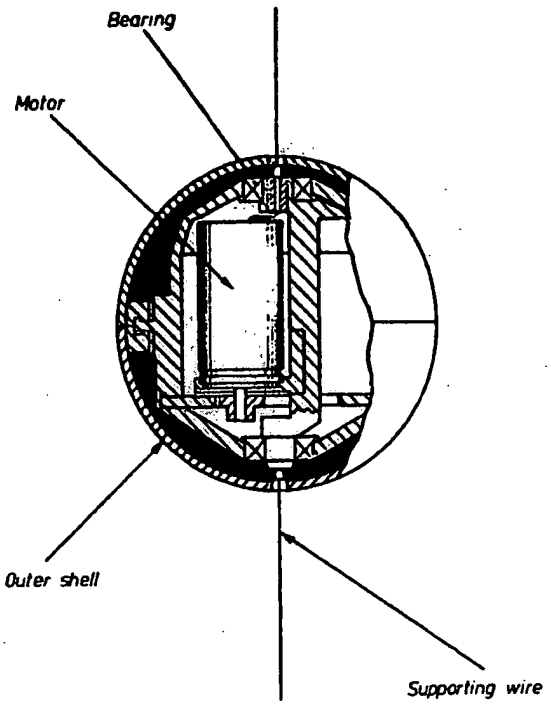

Figure 3 Ball model

2.2 EXPERIMENTAL RESULTS

Initially, in order to investigate the extent of support interference, measurements of C_D were made on a non-rotating smooth sphere. It is known (Goldstein[5] and Achenbach[6]) that the flow about a smooth sphere is highly dependent on Reynolds number and that, over a small Reynolds number range at about $Re = 4 \times 10^5$, the C_D reduces from about 0.45 to 0.1. In the high C_D regime the flow over the ball is laminar and separation occurs just ahead of the point of maximum thickness. The critical Reynolds number, i e the Reynolds number at which the rapid C_D reduction takes place, will occur earlier if the surface of the sphere is rough or the oncoming flow is turbulent. It was anticipated that if the support system seriously interfered with the flow then local regions of disturbed flow would be generated and the C_D would be reduced below the corresponding value given in the literature.

Measurements of C_D for a smooth, hexagonally-dimpled and conventionally-dimpled ball at zero spin are plotted in Figure 4 and it can be seen that the drag of the smooth ball remained high throughout the speed range.

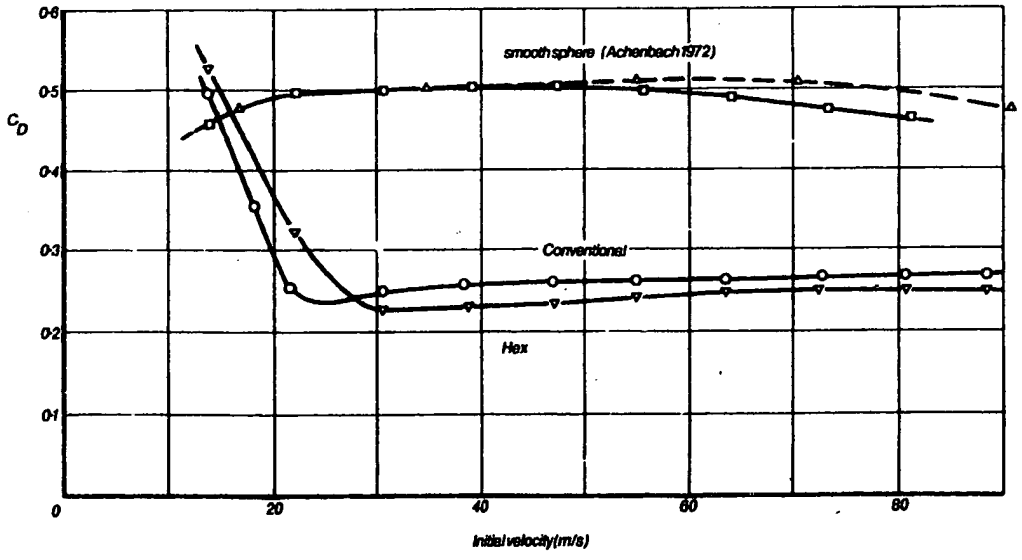

Figure 4 Drag coefficient versus wind speed for zero spin

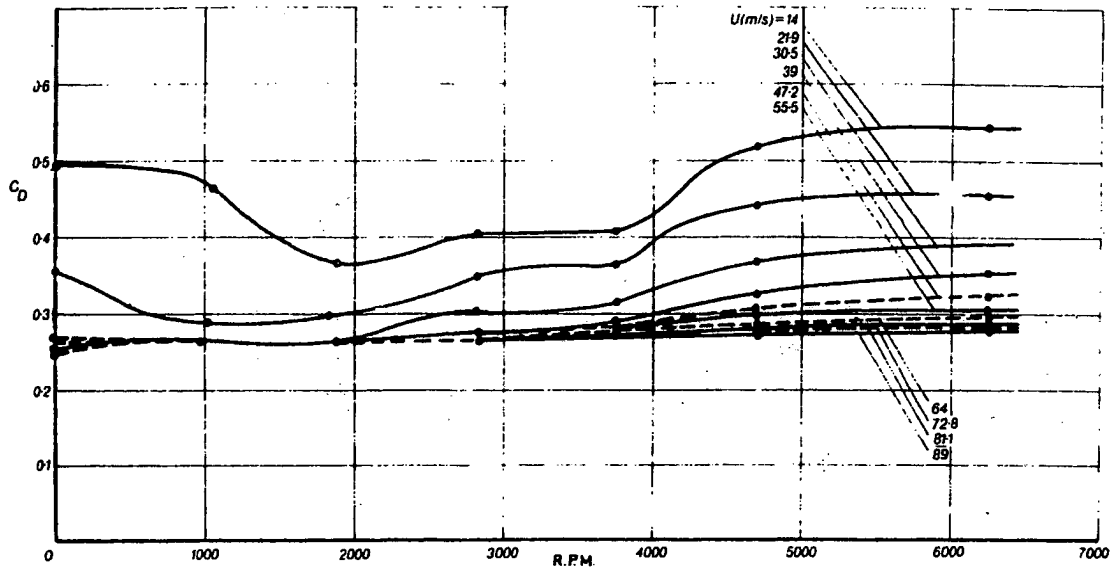

Figure 5 Drag coefficient. Conventional ball

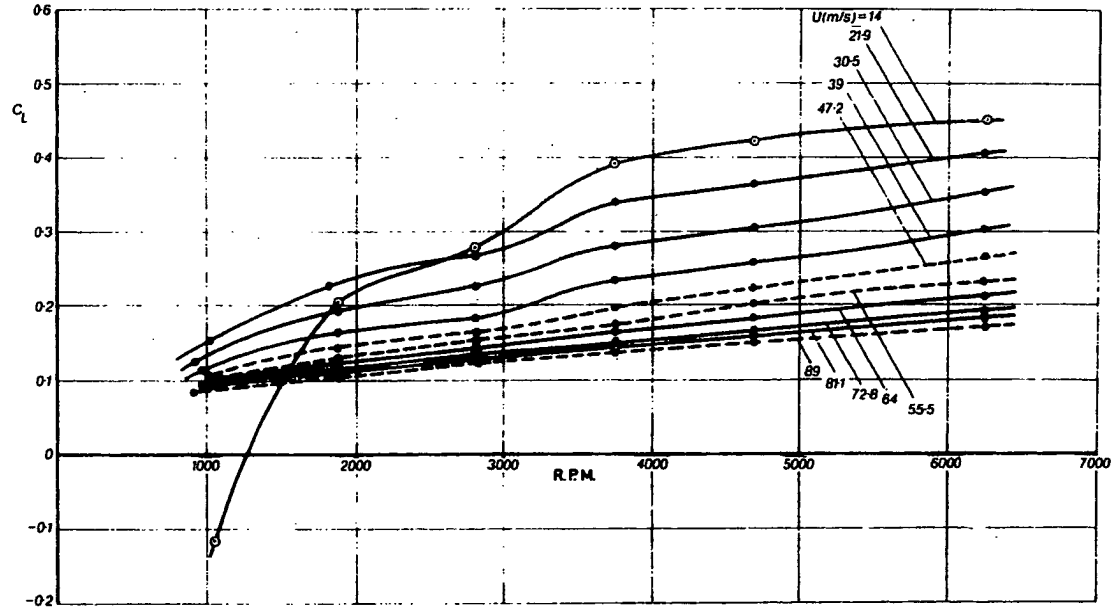

Figure 6 Lift coefficient. Conventional ball

The smooth sphere results are shown to be close to the values of C_D measured by Achenbach[6] and they lie within the general scatter of published data. These results confirm that there was little support interference from the fine suspension wires over the Reynolds number range examined. Initial tests with thicker supports, however, did show a departure of the results from the published data. Clearly the dimpled balls show a critical Reynolds number behaviour and, although the C_D reduction is smaller than that occurring on a smooth sphere, it happens at a lower Reynolds number (see Figure 1). At speeds above about 30 m/s the hexagonally-dimpled ball has a slightly lower C_D than the conventional ball.

It is interesting to compare the variation with Reynolds number of the C_D of a conventionally-dimpled golf ball with the C_D of spheres roughened with sand grains. Achenbach[1] has carried out a series of measurements of C_D for spheres with various ratios of the average diameter of the sand grains k to the sphere diameter. Achenbach's results are shown in Figure 1; it can be seen that increase of k/d reduces the critical Reynolds numb but that after the minimum the C_D rapidly rises, owing to forward movement of the transition point and the artificial thickening of the boundary layer by the roughness elements. It is difficult to compare dimples with sand roughness but presumably a relevant parameter is the ratio of the depth to the ball diameter (i e, $k/d \simeq 900 \times 10^{-5}$. Comparing golf ball C_D values with the results for sand-roughened spheres given in Figure 1, it can be seen that, a the same value of k/d, dimples are more effective at reducing the critical Reynolds number.

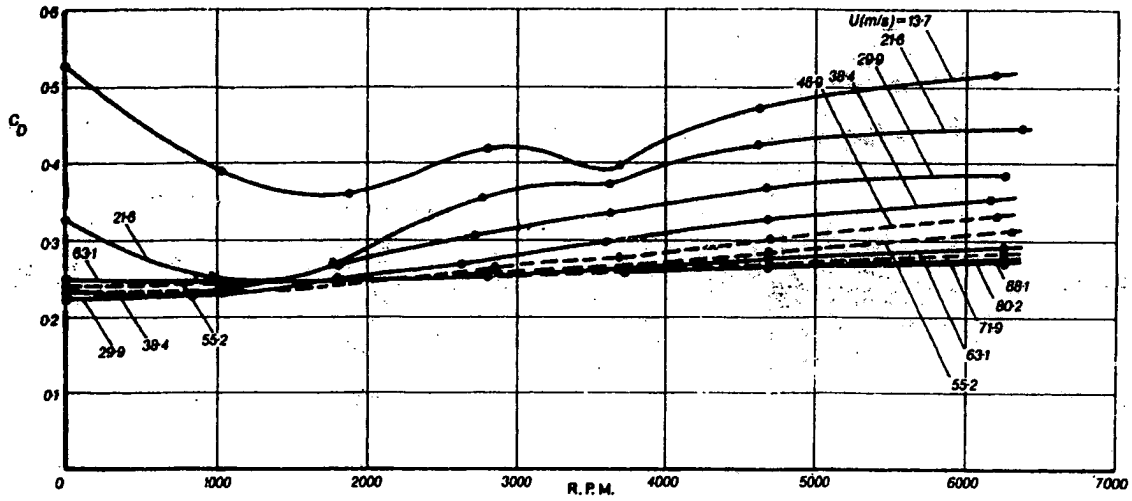

Figure 7 Drag coefficient. Hexagonally-dimpled ball

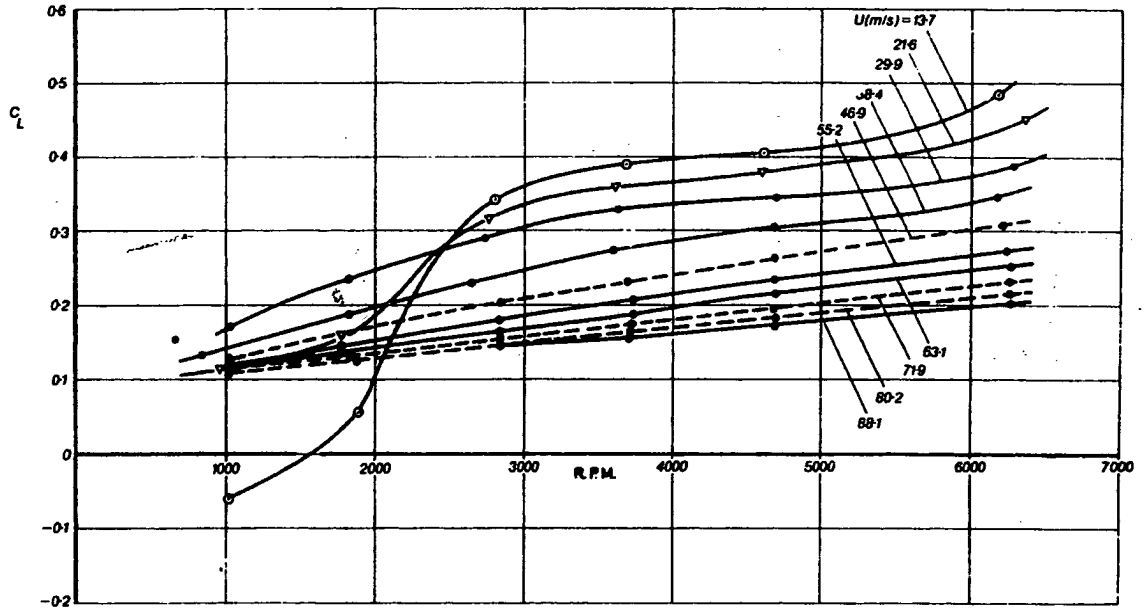

Figure 8 Lift coefficient. Hexagonally-dimpled ball

Another interesting point to note is that the golf ball C_D does not show the rapid increase with Reynolds number after the critical value. This suggests that the dimples are effective in tripping boundary layers without causing the thickening associated with positive roughness. It also suggests that dimples fix the transition point far forward. Clearly then the local flow about the dimples and the dimple shape must be important factors in determining C_D.

Measurements of the lift and drag on both hexagonally-dimpled and conventionally-dimpled balls were made at ten speeds between about 14 and 90 m/s and for six spin rates up to about 6250 rpm. This provides sets of data for the two balls over a wide range of Reynolds number and spin parameter. The variations of C_D and C_L with spin, for the conventional ball, are shown in Figures 5 and 6 respectively, for the ten values of velocity. The corresponding values for the hexagonally-dimpled ball are shown in Figures 7 and 8. In the absence of any gross Reynolds number effect, one would expect C_L to rise with increasing spin and, if one anticipates an induced drag effect similar to that observed with finite aspect ratio wings, C_D would rise. For a given rpm, increase of the velocity will reduce the spin parameter v/U and hence reduce the C_L and the C_D. The results in Figures 5 to 8 show these trends, apart from data taken at low speed at low rpm. In Figures 6 and 8 the lift is seen to be negative at the lowest speed below about 1500 rpm. At the lowest speeds the Reynolds number is below the critical value and the flow over the non-spinning ball is laminar. When the ball is spinning, disturbances first occur in the boundary layer passing over the part of the ball surface that is advancing against the main flow, i e, on what would be the

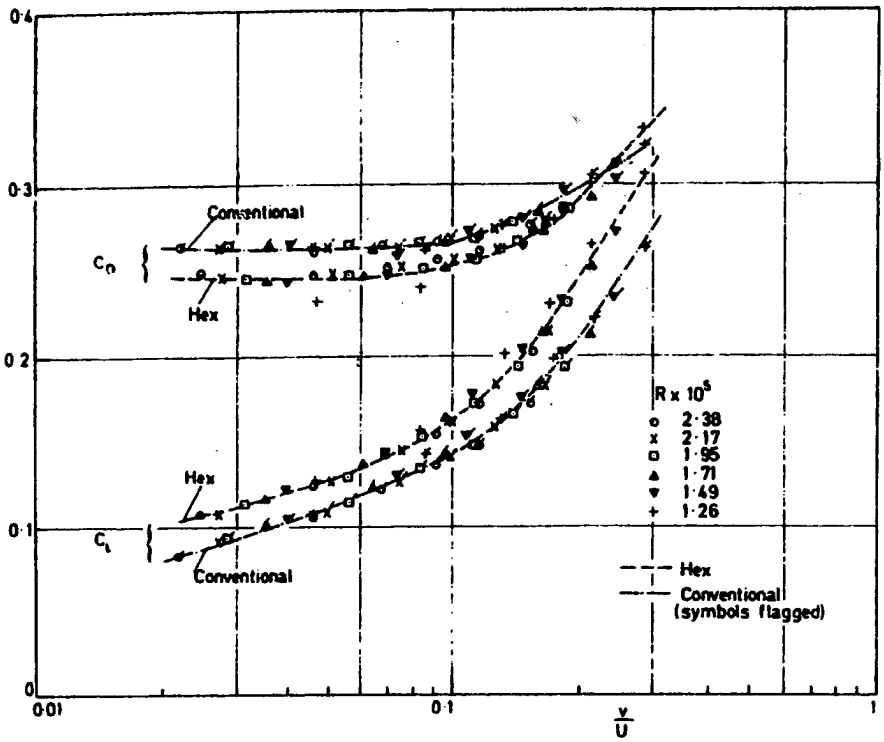

Figure 9 Comparison of conventional and hexagonally-dimpled ball. Re = $1.3 \times 10^5 \rightarrow 2.4 \times 10^5$

underside of the ball. Transition occurs on this side, creating a negative lift force. With further increases in spin or speed, transition occurs on the top of the ball as well and the lift reverts to a positive value. This behaviour has been noted in the flow past rotating cylinders in the critical Reynolds number regime.

Above the critical Reynolds number, increases in rotational speed give a nearly linear increase in lift. However, it is interesting to note that, if the C_L curves are extrapolated back to zero spin, finite values of C_L ($\simeq 0.06$) are indicated rather than the zero value which is, of course, observed. The non-linear behaviour up to about 1000 rpm means that the lift can not be explained by any simple attached flow circulation theory. In order to compare the lift and drag developed by the two different dimple configurations, C_D and C_L values for each ball were plotted against the spin parameter v/U for different Reynolds numbers. The results are shown in Figure 9 for Reynolds numbers between 1.26×10^5 and 2.38×10^5; these correspond to speeds of between about 45 and 88 m/s. The collapse of data from different runs reflects the lack of dependence on Reynolds number and the overall accuracy of the experimental results.

At Reynolds numbers below 1.26×10^5 an effect of Reynolds number begins to appear and a collapse of data on a universal curve is not possible. It can be seen that, as the lift increases, the drag increases and thus a golf ball behaves in the same way as a more conventional lifting body where an induced drag increment is experienced. In general the hexagonally-dimpled ball is superior to the round-dimpled ball, having a higher C_L and a lower C_D, apart from the cross-over of the drag curves at high values of v/U, where C_L becomes very high.

3. Computation of Trajectories

With knowledge of the aerodynamic forces and initial conditions it is possible to compute the complete trajectory for a golf ball drive. The equations of motion are

$$\ddot{x} = -\frac{\rho S}{2m}(\dot{x}^2 + \dot{y}^2)(C_D \cos\alpha + C_L \sin\alpha)$$

$$\ddot{y} = \frac{\rho S}{2m}(\dot{x}^2 + \dot{y}^2)(C_L \cos\alpha - C_D \sin\alpha) - g,$$

where x and y are measured in the horizontal and vertical directions respectively, g is the acceleration due to gravity, m is the mass of the ball and α is the inclination of the flight path to the horizontal, i e, $\alpha = \tan^{-1}(\dot{y}/\dot{x})$. These equations were solved using a step-by-step calculation procedure on a digital computer. All the wind-tunnel data were stored on the computer and at each time step the computer was programmed to interpolate the data to

find the appropriate values of C_L and C_D. The step size chosen corresponded to 0.001 seconds of real flight time and test calculations using various time intervals indicated that the size adopted was sufficiently small and that the absolute error due to the numerical procedure was ±0.01 m on the prediction of range.

In order to compute the drive trajectory the initial spin, launch angle and launch velocity need to be known. A high-speed photographic technique was set up by Uniroyal Ltd to measure these parameters for a number of golfers. The golfers were classified into two groups; professional and amateur. The players repeatedly drove off, and on each occasion launch angle, spin and launch speed were measured. Mean launch parameters for professional and amateur golfers are shown in Table I. The results show that a typical professional drive, apart from being faster, is also at a lower angle and higher spin than a typical amateur drive.

TABLE I

	Spin (rpm)	*Launch angle* (degrees)	*Launch velocity* (m/s)
Professional drive	3450	6.1	68.1
Amateur drive	2450	9.9	56.7

A typical trajectory is shown in Figure 10. The aerodynamic forces lose importance as the flight progresses, since velocity is decreasing and in the second half of the trajectory the only significant force acting is that due to gravity.

Figure 10 Calculated trajectory . Initial conditions: velocity 57.9 m/s, elevation 10°, spin 3500 rpm

The amount by which the spin decays during a flight is not known accurately, although an estimate of the aerodynamic torque was obtained by measuring the electric current needed to rotate the ball in the wind tunnel. This indicated that the decay would be negligible during the part of the flight when the aerodynamic effects dominate. Various realistic spin decay assumptions, including the case where the decay is proportional to the spin squared, were used in the calculation of trajectory but very little dependence was found.

Some results of the computations for the effect of spin rate, initial velocity and initial angle are shown in Figures 11 to 13. Figure 11 shows the effect of spin for an initial velocity of 58 m/s and an initial elevation of 10° These results show that for these initial conditions maximum range is obtained for a spin of about 4000 rpm. Compared with a flight without spin, a spin of 4000 rpm gives about a 90 per cent increase in range. As a further

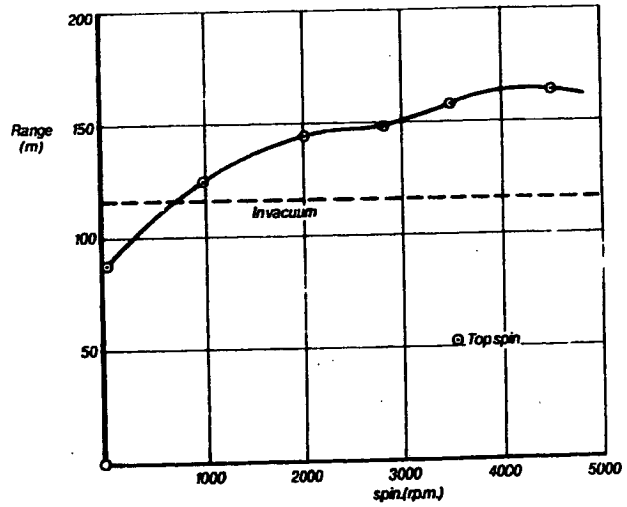

Figure 11 Effect of spin on range . Initial conditions: velocity 57.9 m/s, elevation 10°. Conventional ball

comparison the range for the same initial conditions, but without aerodynamic forces, is shown as the "in vacuum" result. It can be seen that above a quite modest spin rate the aerodynamic lift force helps to carry the ball farther than in the "in vacuum" case. To illustrate the importance of the aerodynamic forces still further, one result is shown in Figure 11 for a drive but with top spin. Changing the sign of the lift force reduces the range by about two thirds.

The effect of varying the initial velocity is shown in Figure 12. At low velocities very little lift is produced and the carry is small, but above 30 m/s the range rapidly increases, the dependence on changes in the initial velocity being almost linear. In practice, hitting the ball harder has the effect of increasing both the initial velocity and spin.

Figure 13 shows how the range is affected by the angle at which the ball leaves the tee. It should be noted that the curve will not pass through the origin since even at zero elevation a lift will be developed which will carry the ball an appreciable distance. The range is still increasing, albeit slightly, at an angle of 15°. This information could be used to indicate what initial spin and launch angle a club should be designed to impart to a ball in order to achieve maximum range. The measurement and computation technique developed could also be used to examine, say, the effects of head or tail winds and the trajectories of other golf shots, such as that from an iron where spin may be much higher.

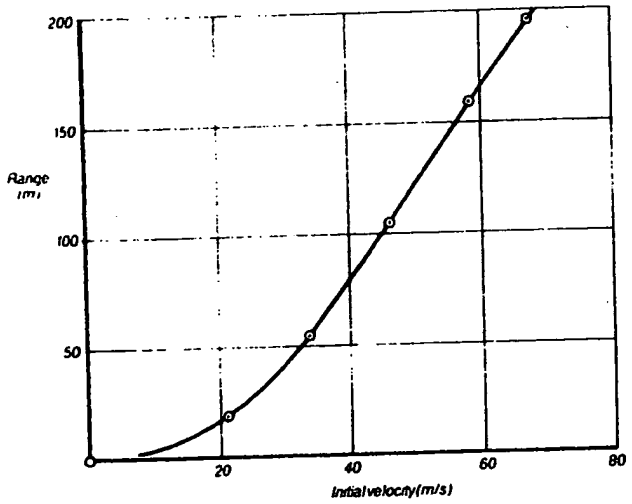

Figure 12 Range for varying initial velocity .
Initial conditions: elevation 10°, spin 3500 rpm. Conventional ball

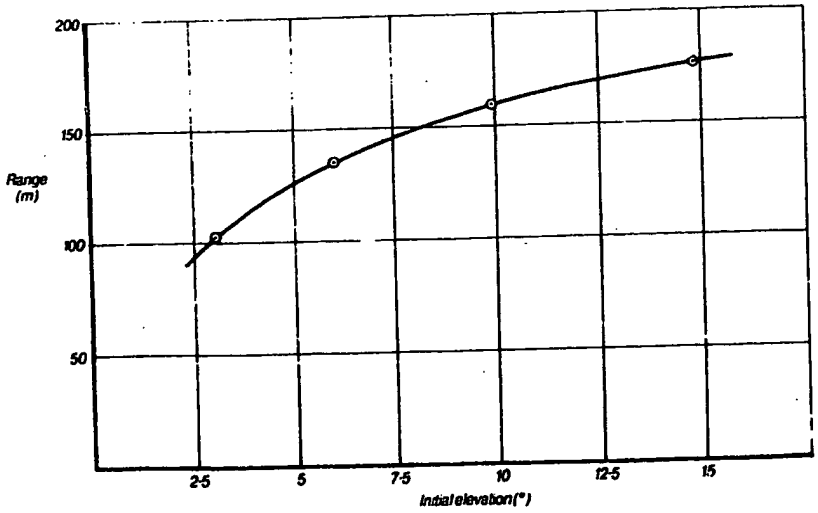

Figure 13 Effect of initial elevation on range .
Initial conditions: velocity 57.9 m/s, spin 3500 rpm. Conventional ball

4. Comparison with Full Scale

The final phase of the investigation was to compare the ranges predicted from the wind-tunnel results with actual measured values using golf balls launched by a driving machine. By using a driving machine the launch conditions can be carefully controlled. These tests were performed by Uniroyal Ltd and we are grateful to them for the data supplied for use in this paper.

Their driving machine can be adjusted such that initial velocity, angle and spin can all be varied and in these tests it was set up to produce conditions typical of golf drives. It was not possible to monitor the complete trajectory but it was possible to mark the landing point and thus record the range. In order to make the comparison with the range computed using the wind-tunnel data, the high-speed photographic technique was again used to measure the launch parameters. Thus the aerodynamic performance is assessed independently of the mechanical properties of the ball.

Comparisons of the measured ranges with the computed ranges for a round-dimpled and hexagonally-dimpled golf ball are shown in Figures 14 and 15 respectively. Each measured range is an average range of nine balls driven twice; however, the scatter on ranges between individual balls was usually small. The corresponding predicted ranges were computed in each case. The agreement between measured and computed results was closest for the hexagonally-dimpled ball with, in most cases, the round-dimpled ball travelling slightly farther than predicted. For given initial conditions, this tends to exaggerate any predicted advantage of the hexagonally-dimpled ball. The driving machine results show the hexagonally-dimpled ball to travel approximately six yards farther than a round-dimpled ball under normal driving conditions.

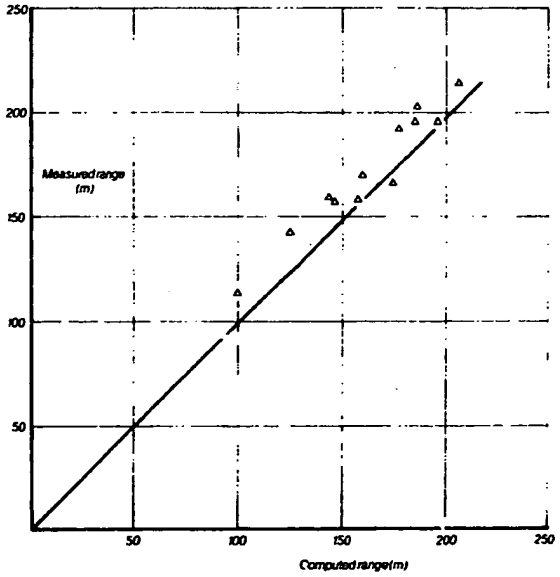

Figure 14 Comparison of measured and predicted range for a golf ball with round dimples

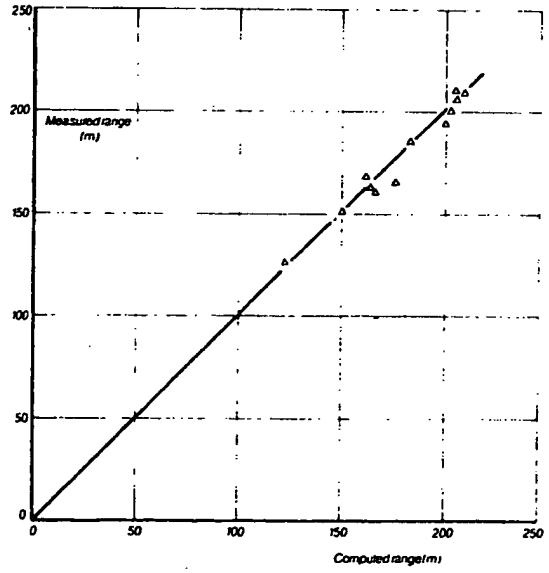

Figure 15 Comparison of measured and predicted range for a hexagonally-dimpled ball

5. Discussion of Results

The aerodynamics of a golf ball depends on the flow induced by the dimples and unfortunately it is difficult to analyse this very closely, especially when the ball is spinning. Clearly they effect transition and reduce the critical Reynolds number below that for a smooth sphere. Unlike sand-roughened spheres, however, the C_D does not rise again immediately beyond the critical Reynolds number region. Probably sand roughness has the effect of thickening the turbulent boundary layer and thus making it less able to remain attached, whereas the dimples appear to act as more efficient trips. Hexagonal shaped dimples act as even more efficient trips than round dimples, perhaps by shedding into the boundary layer more discrete vortices from their straight edges. A detailed flow investigation of dimple flow is needed before more definite conclusions can be drawn.

Comparison of the measurements of C_D and C_L presented here with those of Davies[3], made at a Reynolds number of about 0.9×10^5, shows that he was in a regime where the flow was still weakly dependent on Reynolds number. His measurements of C_D are higher than ours whereas his measurements of C_L are slightly lower;

otherwise the trends are the same. Williams[4] deduces, from measured ranges, that $C_D = 151/V$, where V is the initial ball velocity in m/s, by assuming that flight does not depend on lift or spin. These assumptions are not supported by the findings of this research and his relation for C_D does not fit the data.

The superior aerodynamic performance of the hexagonally-dimpled ball suggests that, for the same launch conditions, it should travel farther than a round-dimpled ball. This was borne out by driving machine tests, although the advantage of the hexagonally-dimpled ball was not as great as that suggested by the wind-tunnel experiments. This was due to an under-prediction of range for the conventional ball, the predictions for the hexagonally-dimpled ball being very close to the measurements. Both balls were constructed using golf ball mould drawings and no attempt was made to model the coating applied to a finished ball. This will mean that the dimple edge radius may not be truly scaled and this may be an important parameter in determining C_D and C_L. More work is required to examine the effect of edge radius on the aerodynamic performance.

6. Conclusions

A wind tunnel has been used to measure the lift and drag acting on golf ball models over a wide range of Reynolds number and spin rate. The effect of changing the dimple shape from round to hexagonal has been examined. The dimples trip the boundary layer and induce an earlier critical Reynolds number. The hexagonally-dimpled ball showed a superior aerodynamic performance compared with a round-dimpled ball.

Using the aerodynamic data, ranges were computed for various initial conditions and the effects of initial velocity, angle and spin were investigated separately. Comparisons with full-scale data from a driving machine showed that the hexagonally-dimpled ball range was closely predicted whereas the round-dimpled ball range tended to be slightly under-predicted, possibly owing to minor model inaccuracies. With the data presented in this paper the influence of the aerodynamic forces on a wide range of golf shots can be analysed.

This investigation has, at the same time, highlighted the effectiveness of dimples as a method of causing early boundary-layer transition without the drag penalties associated with other generally accepted trips which protrude from the surface.

Acknowledgements

The authors wish to acknowledge the help given by Messrs Uniroyal Ltd, and in particular by Dr T Moore, who very kindly provided us with the range data referred to in this paper. We are also indebted to Dr M E Davies for his assistance with the computer calculations.

References

1. E Achenbach — The effects of surface roughness and tunnel blockage on the flow past spheres. *Journal of Fluid Mechanics*, Vol 65, p 113, 1974.

2. J Maccoll — Aerodynamics of a spinning sphere. *Journal of the Royal Aeronautical Society*, Vol 32, p 777, 1928.

3. J M Davies — The aerodynamics of golf balls. *Journal of Applied Physics*, Vol 20, p 821, 1949.

4. D Williams — Drag force on a golf ball in flight and its practical significance. *Quarterly Journal of Mechanics and Applied Mathematics*, Vol XII, p 387, 1959.

5. S Goldstein (Editor) — *Modern Developments in Fluid Dynamics*, p 16. Clarendon Press, Oxford, 1938.

6. E Achenbach — Experiments on the flow past spheres at very high Reynolds numbers. *Journal of Fluid Mechanics*, Vol 54, p 565, 1972.

Evidence Appendix E
U.S. Patent Number 4,501,214 to Meyer

This reference was originally entered in the record by the Primary Examiner in an Office Action mailed December 28, 2005.

This Page is Inserted by IFW Indexing and Scanning Operations and is not part of the Official Record

BEST AVAILABLE IMAGES

Defective images within this document are accurate representations of the original documents submitted by the applicant.

Defects in the images include but are not limited to the items checked:

- ❑ BLACK BORDERS
- ❑ IMAGE CUT OFF AT TOP, BOTTOM OR SIDES
- ❑ FADED TEXT OR DRAWING
- ❑ BLURRED OR ILLEGIBLE TEXT OR DRAWING
- ❑ SKEWED/SLANTED IMAGES
- ❑ COLOR OR BLACK AND WHITE PHOTOGRAPHS
- ❑ GRAY SCALE DOCUMENTS
- ❑ LINES OR MARKS ON ORIGINAL DOCUMENT
- ❑ REFERENCE(S) OR EXHIBIT(S) SUBMITTED ARE POOR QUALITY
- ❑ OTHER: _____

IMAGES ARE BEST AVAILABLE COPY.
As rescanning these documents will not correct the image problems checked, please do not report these problems to the IFW Image Problem Mailbox.